The definitive publisher version is available online at https://doi.org/10.1016/j.jwpe.2021.102534

Recent advances in circular bioeconomy based clean technologies for sustainable environment

Lijuan Deng[1], Huu Hao Ngo[1,2,*], Wenshan Guo[1], Soon Woong Chang[3], Dinh Duc Nguyen[3], Ashok Pandey[4], Sunita Varjani[5], Ngoc Bich Hoang[2]

[1]*Centre for Technology in Water and Wastewater, School of Civil and Environmental Engineering, University of Technology Sydney, Sydney, NWS 2007, Australia*
[2]*NTT Institute of Hi-Technology, Nguyen Tat Thanh University, Ho Chi Minh City, Viet Nam*
[3]*Department of Environmental Energy Engineering, Kyonggi University, 442-760, Republic of Korea*
[4]*Centre for Innovation and Translational Research, CSIR-Indian Institute of Toxicology 12Research, Lucknow-226 001, India*
[5]*Gujarat Pollution Control Board , Gandhinagar – 382 010, Gujarat, India*

*Corresponding author: Email: ngohuuhao121@gmail.com

Abstract

The term “circular bioeconomy-based clean technologies” has attracted global attention in recent years, and it now plays an important role in solving issues of increasing biowaste generation, resource scarcity and climate change. This is in line with creating a sustainable environment. Regarding circular bioeconomy-based technologies, wastewaters and solid biowastes are treated as potential and renewable feedstocks for producing value-added resources and bioenergy. Bioelectrochemical systems (BESs) are promising technologies for the treatment of wastewater and conversion of wastes to bioenergy and resources by microbial fuel cells (MFCs) and microbial electrolysis cells (MECs). Biowastes from various sectors, including organic fraction of municipal solid waste, agricultural residues, animal manure, food wastes and sewage sludge, can be converted to biochar, biofuel and other valuable products via thermochemical technologies. This research explains some representative circular bioeconomy based technologies for the treatment of wastewater and biowastes while focusing on the impact of these technologies and products on environmental sustainability.

Keywords: Circular bioeconomy; Bioelectrochemical systems; Thermochemical technologies; Nutrient recovery; Biochar; Bioenergy

1. Introduction

Economic development and the world’s growing population are accelerating demand for energy, but all this is doing is accelerating the exhaustion and scarcity of non-renewable natural resources (i.e., fossil fuels, minerals), producing enormous amounts of waste, and adding to climate change. This scenario in turn produces serious ecological and socioeconomic challenges [1]. It has been reported that global resources consumption has increased by 17.4% from 2010, reaching 85.9 billion metric tons in 2017 [2]. Global food waste in cities will increase to 138 million tons by 2025

[3]. Total amounts of global municipal solid waste are predicted to be 3.4 billion tons in 2050 [4]. In 2020, the global average temperature was 1.2 °C above the pre-Industrial Revolution baseline due to rising global greenhouse gas (GHG) emissions. This has led to 91.3 mm of global mean sea level above the value in 1993 [2, 3]. For this reason, it is imperative to introduce sustainable development (consumption and production), in order to use resources, energy and infrastructure in more efficient and viable ways [5]. Circular bioeconomy is now a promising method of sustainable development to generate value-added products such as clean water, nutrient, biofuel, biomethane, biochar from renewable biological resources (i.e. wastewater, biowastes) and conserve the long-term value of resources through effective conversion biotechnologies. This can achieve zero waste generation, curtail GHG emissions, reduce dependence on fossil fuels, and save environmental and economic costs [6, 7].

Bioelectrochemical systems (BES) have increasingly attracted much more attention as a sustainable waste-to-energy technology and in parts of the circular bioeconomy, wastewater can be treated to produce high quality water and employed as feedstock for bioelectricity and bioenergy generation [8]. Microbial fuel cells (MFCs) are mainly used for electricity production by oxidizing organic matter (i.e. acetate) by electrogenic bacteria on the anode (biotic anode) and reducing oxygen at the cathode at neutral pH. They are operated without external potential due to the occurrence of spontaneous bioelectricity production by the anodic biofilm. Microbial electrolysis cells (MECs) derived from modification of MFC requiring an external power source is generally adopted for storing electrical energy as a biofuel (i.e., H_2, CH_4) [9, 10]. In addition to nutrient removal/recovery, BES has been widely applied in the treatment of wastewater containing different types of emerging pollutants, i.e. dye compounds, aromatic hydrocarbons, petroleum hydrocarbons, trichloroethene, etc., which simultaneously generate electricity [11].

Biowastes (including sewage sludge, agricultural residues, municipal solid waste, food wastes and animal manure) contain heating values or energy content (higher heating value (HHV)), i.e. 15-20 MJ/kJ for dry sludge, 10.87 MJ/kg for cattle manure, 19.72 MJ/kg for palm kernel shell, 17.0 MJ/kg for mixture of discarded vegetables and fruits [12-15]. Moreover, sewage sludge obtained from primary and secondary treatment stages in wastewater treatment plants (WWTPs) is rich in nitrogen and phosphorus. Hence, biowastes can be considered as potential source of energy and a good option to replace conventional fossil fuels to accomplish waste-to-energy and nutrient recovery approaches [12]. Thermochemical conversion, including pyrolysis, hydrothermal carbonization, torrefaction, hydrothermal liquefaction and gasification, converts biowastes into high-value added products (solid fuel, liquid fuel, biochar/hydrochar, etc.) and greater volume reduction of biowastes. Solid and liquid fuel can be used as surrogate fuel [16-19]. Biochar or hydrochar can be applied in soil amendment, organic waste composting, and removals of emerging pollutants, air pollutants and heavy metal [17, 20-22].

In recent years, some review papers focused on the developments and applications of BES for removing pollutants from wastewater [1, 9], BES for resource recovery and limitations for wide applications [23], positive effects of BES on performance of anaerobic digestion [24]. BES-based hybrid systems have been also reviewed in these years, such as BES integrated with aerobic/anaerobic treatment systems, specifically anaerobic digestion, aerobic tanks, etc., for sustainable wastewater treatment [25], methane upgrade [26], and modified BES (i.e., osmotic microbial fuel cell (OsMFC), MFC coupled with osmotic MBR (MFC-OMBR), etc.) for resource recovery [27]. Nevertheless, the applications of BES for wastewater treatment and energy recovery are still the focus of many current studies. Conversely, thermochemical conversion of biowastes was reviewed with respect to different approaches, techno-economic and bibliometric analysis [16], thermochemical conversion of sewage sludge [19, 28, 29, 30], and engineered activated

biochar from microwave pyrolysis process and its applications [18]. However, we lack review papers about thermochemical conversion of different types of biowastes and effects of products on environmental sustainability. It is imperative to provide a review on current research progress. This review article aims to update studies on development and applications of BES for wastewater treatment and resource recovery, and conversion of biowastes to high value-added products by thermochemical technologies using the circular bioeconomy concept.

2. Bioelectrochemical systems (BES) for wastewater treatment and resource recovery

2.1. Biogas upgrading from wastewater

Currently, BES have been used for reducing CO_2 mainly captured into or dissolved in wastewater and biogas upgrading. This is done by converting CO_2 to biomethane using electrons enriched with methanogens and/or employing electro-active microbes as biocatalysts. Microbial electromethanogenesis (EMG) could occur with a biocathode containing methanogens for methane generation, in which direct EMG used the cathode for direct reduction of power source and indirect EMG employed H_2 as electrochemical mediator. Compared to indirect EMG, direct EMG was more energy-efficient [31]. Thus, a membrane-less medium-scale EMG-BES prototype was developed for simultaneous wastewater treatment in the anodic chamber and reduction of CO_2 to CH_4 in the cathodic chamber at pH = 7 [10]. When using acetate as medium, generation of electrons took place in abiotic anode (Eq. (1)) and/or biotic anode (Eq. (2)), along with acetoclastic methanogenesis (Eq. (3)). In the cathodic chamber, direct EMG dominated the cathode to generate CH_4 (Eq. (4)) when the applied voltage was less (0.1-0.2 V). After increasing voltage (0.6 V < voltage < 1 V), indirect EMG would occur for CH_4 generation (Eq. (5)) (SHE = standard hydrogen electrode):

$$2H_2O \rightarrow O_2 + 4H^+ + 4e^- \text{ (voltage of +0.82 V vs SHE)} \quad (1)$$

$CH_3COO^- + 4H_2O \rightarrow 2HCO_3^- + 9H^+ + 8e^-$ (biotic acetate oxidation; voltage -0.28 V vs SHE) (2)

$CH_3COO^- + H^+ \rightarrow CO_2 + CH_4$ (acetoclastic methanogenesis) (3)

CO_2 (dissolved) + $8H^+ + 8e^- \rightarrow CH_4 + 2H_2O$ (direct EMG; potential -0.244 V vs SHE) (4)

$2H^+ + 2e^- \rightarrow H_2$ (5)

$CO_2 + 4H_2 \rightarrow CH_4 + 2H_2O$ (hydrogenotrophic methanogenesis; indirect EMG; potential -0.41 V vs SHE) (6)

The applied voltages could enhance activities and growth rates of exoelectrogenic bacteria at the anode and hydrogenotrophic methanogens at the cathode over the acetoclastic methanogens. It should be noted that the applied voltage must be optimized. Relatively high voltage stimulates biofilm formation and enhances microbial activity. However, the extremely high voltages will suppress the electrochemically active bacteria [10, 32]. At the applied voltage of 0.7 V and 32 °C, CH_4 production rate and organic matter removals reached 4.4 $L/m^2 \cdot d$ and around 70% with current density of 0.5 A/m^2, respectively. Moreover, the high CH_4 content in biogas (around 87%) was close to biomethane standards. Even when decreasing temperature to 25 °C, CH_4 content in biogas was high around 90% with higher electro-active bacteria growth than acetoclastic methanogens, despite that CH_4 production declined by 33%.

Overall, the EMG-BES could ensure the stable biological process (reduction of acid regression by acetate oxidation at the anode), generation of high-quality biogas (> 87% of CH_4 content, close to biomethane standards) and possibility of low-temperature operation [10]. To reduce CO_2 emissions from anaerobic digestion of sewage sludge, membrane contactors was used for CO_2 capture into wastewater, which was coupled with EMG-BES reactors for bioconversion of the dissolved CO_2 to CH_4. NaOH solution was employed in membrane contractors to increase the alkalinity of wastewater, thus accelerating chemical adsorption process. During the process, around

155 0.3-3.7% of the injected CO_2 in wastewater was converted to CH_4 and CH_4 production was as high
156 as 4.6 L/m^2·d at higher applied voltage of 4.0 V [32].

157 Batlle-Vilanova [33] also found that the BES containing biocathode enriched with some
158 methanogens (i.e. *Methanobacterium* sp.) had potential in transforming CO_2 from wastewater
159 (effluent from a water scrubbing-based biogas upgrading process (ABAD Bioenergy™ an
160 European Patent) in WWTPs) into CH_4 (Eq. (4)). Additionally, chlorine could be generated in the
161 anode when using brine as anolyte:

162 $2Cl^- \rightarrow Cl_2 + 2e^-$ (E^o = 1.6 V vs SHE) (7)

163 $2H_2O \rightarrow O_2 + 4H^+ + 4e^-$ (E^o = 1.23 V vs SHE (8)

164 The application of this technology in wastewater treatment by WWTPs in a real case scenario
165 increased biomethane generation in biogas by 17.5%, reduced CO_2 emissions by 42.8% and
166 produced more than 60 ppm of chlorine for disinfection of all the treated wastewater.

167

168 **2.2. Nutrient removal and recovery**

169 In BES, organic matters (i.e., acetate, glucose) as electron donor are oxidized by anaerobic
170 bacteria or electrochemically active bacteria (EAB) on the anode acting as electron acceptor, which
171 generates electrons and protons. Partial oxidation of NH_4^+-N at the anode also releases the
172 electrons. The electrons are moved to the anode via extracellular electron transport mechanisms
173 and subsequently transferred to the cathode through the external electric circuit. Besides,
174 dissimilatory nitrate reduction to ammonia (DNRA) could also occur on the anode in MFC when
175 C/N ratio in the range of 8.0-0.5 and low external resistance of 10 or 100 Ω, or in MEC at relatively
176 high C/N ratio of 8.0 and low applied voltage of 0.5 V [34]. Ammonia in gas phase obtained after
177 stripping employing aeration in cathodic chamber of MFC or nitrogen gas generated in cathodic

chamber of MEC can be recovered as ammonium sulfate (NH_3SO_4) by diluted sulfuric acid, liquid ammonia, or ammonium biocarbonate (NH_4HCO_3) by CO_2 [35].

Generally, nitrogen (including ammonium (NH_4^+-N), nitrite (NO_2^--N), nitrate (NO_3^--N)) removal occurs via anoxic anammox process or anoxic ammonium oxidation on the bioanode and via cathodic denitrification process on the cathode/biocathode in MFC (Fig. 1). Cationic exchange membrane (CEM) as separator in MFC inhibited direct transfer of anions and promoted the direct transfer of protons (H^+) and cations (NH_4^+). This favored the increase in pH in the cathodic chamber. The aeration in the cathodic chamber also increased pH in cathodic chamber (8.0-10) due to hydroxide ions generated through oxygen reduction reaction (ORR). Consequently, nutrient recovery could be realized by chemical precipitation (NH_4^+ and PO_4^{3-} precipitating with Mg^{2+} and/or Ca^+ ions). When directly feeding the cathodic chamber by the effluent from anodic chamber, both NH_4^+-N and PO_4^{3-}-P could transfer to the cathodic chamber. As a result, more than 90% of nitrogen and phosphorus recovery was obtained in MFC [36].

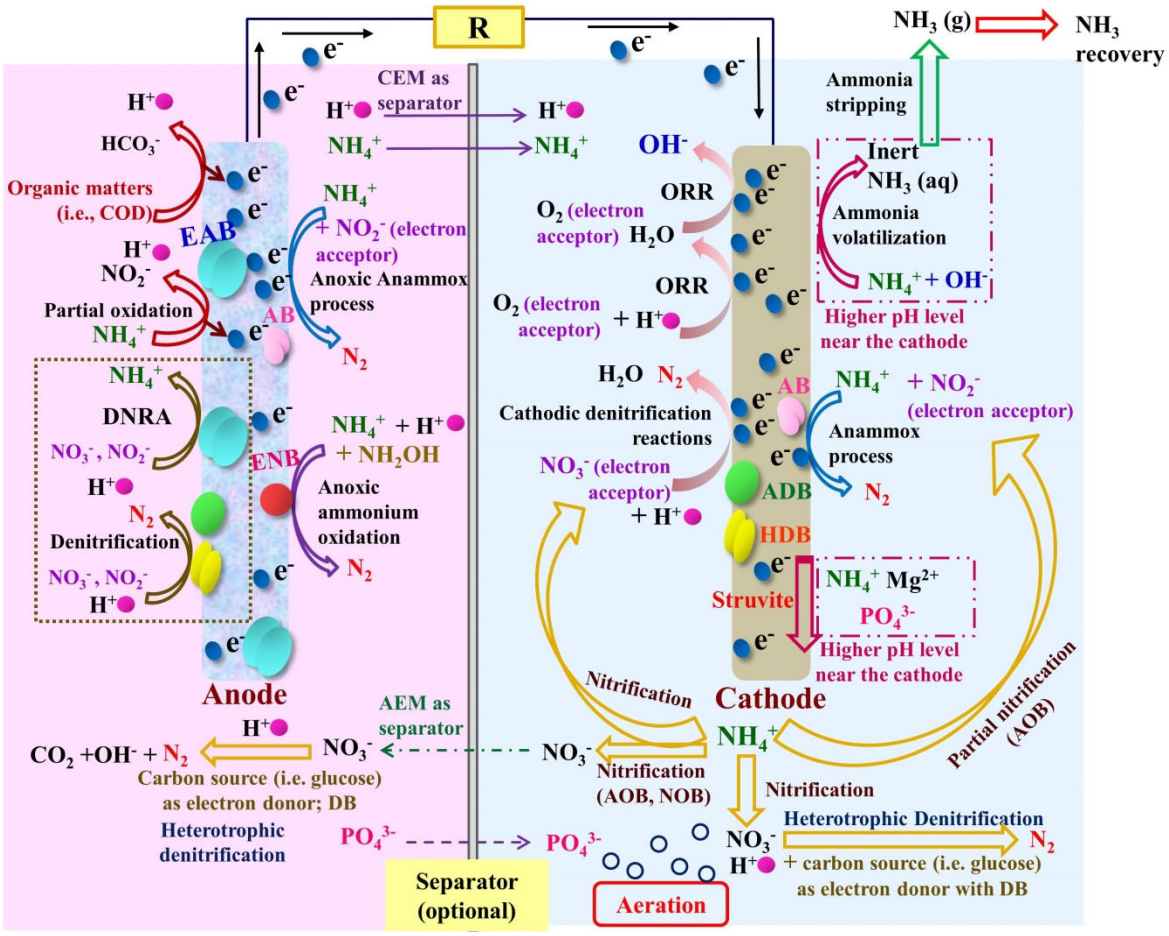

192

193 **Fig. 1.** Possible nutrient removal and recovery pathways in MFC based on information from Wan
194 et al. [34], Nancharaiah et al. [35], Ye et al. [36], Elmaadawy et al. [37], Guo et al. [38] and Lu et
195 al. [39] (Separator is optional (CEM or AEM); Cathodic denitrification reactions include abiotic
196 cathodic reaction (NO_3^- as electron acceptor) and/or biotic cathodic reaction (autotrophic
197 denitrification with biocathode as electron donor autotrophic and heterotrophic denitrification
198 employing organic matters as electron donors)) Note: ADB, Autotrophic denitrifying bacteria;
199 AEM, anion exchange membrane; DB, denitrifying bacteria; DNRA, dissimilatory nitrate
200 reduction to ammonia; EAB, electrochemically active bacteria; ENB, Electroactive nitrifying
201 bacteria; HDB, Heterotrophic denitrifying bacteria; R, Resistor

202

In MFC, NH_4^+-N removal on the bioanode is significantly affected by COD and NH_4^+-N concentrations and COD/NH_4^+ ratio in the feedwater. Microbial population and activity on bioanode increased at higher COD concentrations (i.e. 500-10,000 mg/L, corresponding to COD/ NH_4^+-N ratios of 3.3-66.6), which led to more NH_4^+-N degradation. When increasing NH_4^+-N concentration from 200 to 650 mg/L at fixed COD level (10,000 mg/L), more NH_4^+-N was adsorbed by microbes, but the subsequent biodegradation of NH_4^+-N declined owing to the decreased COD/NH_4^+ ratios from 50 to 15. On the other hand, the higher NH_4^+-N level increased current density and power generation through improving bacterial activity in bioanode at low COD/NH_4^+-N ratio (i.e. 15) and transfer of NH_4^+-N through CEM to the cathodic chamber. At high COD/NH_4^+-N ratio (i.e. 66.6 at COD concentration of 10,000 mg/L, 50 at NH_4^+-N concentration of 200 mg/L), NH_4^+-N removal reached maximum level (91-92%) via biodegradation [40]. In cathodic chamber, a moderate aeration rate favors ammonia recovery and energy saving. When compared to extremely lower and higher aeration rates, the relatively low aeration rate not only maximized ammonia recovery rate (average 7.1 kgN/m^2·d at 100 mL/min vs 1.2-7.1 kgN/m^2·d at 30, 50 and 300 mL/min), but also minimized the energy consumption (average 4.3 kWh/gN at 100 mL/min vs 4.1-6.9 kWh/gN at 30, 50 and 300 mL/min required for removal; average 4.9 kWh/gN at 100 mL/min vs 5.7-26.2 kWh/gN at 30, 50 and 300 mL/min for recovery). Higher ammonia recovery (recovery rate, 7.1 gN/m^2·d) and lower energy consumption (5.7 kWh/kgN) could also be obtained at lower external resistance of 1 Ω due to higher current generation compared with higher external resistance (recovery rate of 3.2-5.0 gN/m^2·d and energy consumption of 6.6-7.2 kWh/kgN at 10 and 100 Ω) [41].

In MEC, cathodic denitrification, partial denitrification, anammox processes and hydrogen gas (H_2) generation occur in the cathodic chamber, which increases cathodic pH and further phosphorus recovery via precipitation. The generation of H_2 in cathodic chamber encourages ammonia

227 removal, which prompts higher NH_4^+-N removal (Fig. 2). In single-chamber membrane-free MEC,
228 the applied voltage (0.2 V) could enhance activity of microbes on electrodes and denitrification via
229 electric stimulation. Moreover, anammox process and autotrophic denitrification were also
230 improved by the current stimulation (69.4% higher nitrogen removal rate than that in the open
231 circuit). This reduced the requirement of carbon source in the feedwater [43]. Compared to MFC,
232 the increased current densities induced by the electric field in MEC enhanced NH_4^+ transfer and its
233 removal [45].
234

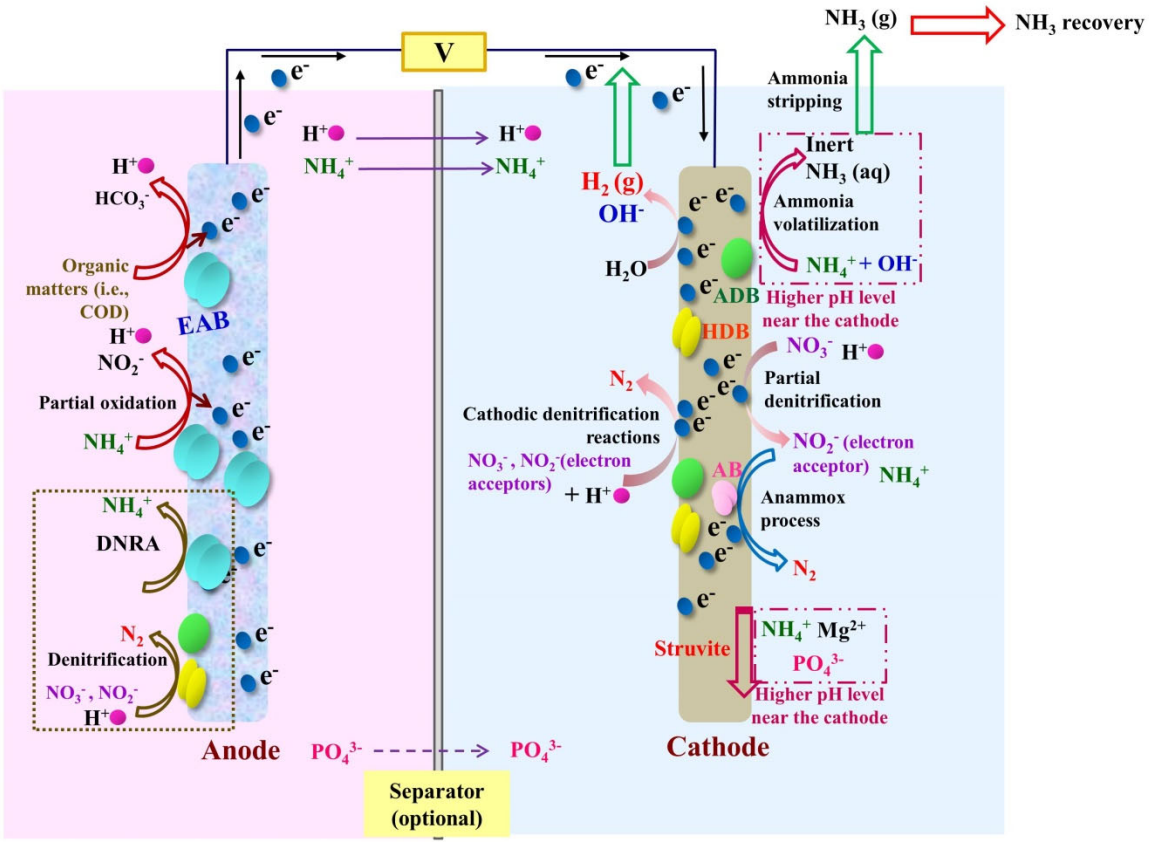

235

236 **Fig. 2.** Possible nutrient removal and recovery pathways in MEC based on information from Wan
237 et al. [34], Nancharaiah et al. [35], Almatouq and Babatunde [42], Xu et al. [43] and Zeppilli et al.
238 [44] (Separator is optional (CEM, AEM or PEM); Cathodic denitrification reactions include
239 abiotic cathodic reaction (NO_3^- as electron acceptor) and/or biotic cathodic reaction (autotrophic

denitrification with biocathode as electron donor autotrophic and heterotrophic denitrification employing organic matters as electron donors)) Note: ADB, Autotrophic denitrifying bacteria; AEM, anion exchange membrane; DB, denitrifying bacteria; EAB, electrochemically active bacteria; ENB, Electroactive nitrifying bacteria; HDB, Heterotrophic denitrifying bacteria; PEM, proton exchange membrane; V, External power (voltage)

COD/N and applied voltage values should be taken into account when operating MEC. The elevated COD/N (NO_3^--N, NO_2^--N, NH_4^+-N) ratio accelerated growth of heterotrophic denitrifying microorganisms, thereby increasing total nitrogen removal rate (695.6 gN/m^3d at COD/N of 2 vs 514.5 $gN/m^3 \cdot d$ at C/N of 1) [43]. pH value in cathodic chamber increased from 8 to 9.1 when increasing applied voltage (0.4-0.8 V). However, much higher voltage (1.2 V) inhibited bacterial activity, extended cycle duration, decreased pH and phosphorus precipitation rate. Overall, the maximum precipitation rate was obtained (95%) at moderate applied voltage of 1.1 V [42]. Moreover, the low external voltage could reduce energy consumption due to higher current generation compared with higher external voltage (i.e. energy consumption for ammonia recovery, 4.5 kWh/kg N recovery at 0.5 V vs 6.4 kWh/kg N recovery at 0.8 V) [41].

Currently, a three-chamber MEC was constructed to recover nitrogen (i.e. NH_4^+-N) and remove CO_2 from syngas by transfer and separation of different cationic and ionic species driven by the electric field [44]. The MEC consisted of a middle anodic chamber between two cathodic chambers with an anionic exchange membrane (AEM) and CEM as separators (AEM-cathode and CEM-cathode, respectively). During the operational process, influent containing COD and NH_4^+-N fed the anodic chamber. Meanwhile, gas mixture (N_2/CO_2 (70/30 v/v)) flushed through the two cathodic chambers with separators of CEM and AEM in sequence. The overflow of liquid phase from the cathodic chamber with CEM was recirculated between two cathodic chambers every day.

The daily overflow helped to remove NH_4^+-N, leading to nitrogen removal rates of 96 mgN/d (removal of 65%) at anodic potential of + 0.2 V vs SHE and 43 mgN/d (removal of 30%) at anodic potential of -0.1 V vs SHE. CO_2 was mainly removed through sorption as HCO_3^- in the cathodic chamber by the daily overflow (removal of 63% during +0.2 V vs SHE) or transfer of HCO_3^- from cathodic chamber with AEM to the anodic chamber (removal of 49% during -0.1 V vs SHE). Reduction of CO_2 to methane in the cathodic chambers only contributed to 16-20% of CO_2 removal. Moreover, the biogas obtained would not be contaminated by ammonia since AEM reduced the NH_4^+-N concentration in the cathodic chamber.

Human urine contains different types of components, such as urea, inorganic salts (i.e. chloride, potassium, sodium), ammonia, creatinine, phosphate, sulfur, etc. Thus, it can also be used for nutrient recovery by BES. Urea is hydrolyzed in the anodic chamber [38, 45]:

$$NH_2(CO)NH_2 + 2H_2O \rightarrow NH_3 + NH_4^+ + HCO_3^- \quad (9)$$

Then the dissolved ammonia (NH_3) and NH_4^+-N are oxidized into NO_2^--N and NO_3^--N and/or anaerobically oxidized to N_2 via anammox reaction, along with release of electrons. Additionally, biodegradation of organic matters in the wastewater (sodium acetate, creatinine and histidine) also generates NH_3 and electrons [38, 45]:

$$\text{Organic matters} \rightarrow CO_2 + NH_3 + \text{intermediates} + H^+ + e^- \quad (10)$$

Nitrogen removal can be realized in the cathodic chamber as shown in Figs. 4 and 5. The high pH in the cathodic chamber could induce formation of precipitates in different forms, including struvite, hydroxyapatite or calcite [45]:

$$Mg^{2+} + NH_4^+ + PO_4^{3-} + 6H_2O \rightarrow MgNH_4PO_4{\cdot}6H_2O \text{ (struvite)} \quad (11)$$

$$5Ca^{2+} + 3PO_4^{3-} + OH^- \rightarrow Ca_5(PO_4)_3(OH) \text{ (hydroxyapatite)} \quad (12)$$

$$Ca^{2+} + CO_3^{2-} \rightarrow CaCO_3 \text{ (calcite)} \quad (13)$$

Single-chamber air-cathode MFC could remove up to 84% of total nitrogen from urea at high total ammonia nitrogen (TAN) concentration (2630 mg/L) via direct ammonia oxidation near the cathode and anammox process on the anode in series [46]. To simultaneously recover nutrient, sulfur and salts from urine-containing wastewater, a three-chamber resource recovery MFC (RRMFC) was set up, which contained an anodic chamber, a middle chamber and a cathodic chamber with a CEM and an AEM as separators between two consecutive chambers, respectively [38]. The effluent from anodic chamber directly fed cathodic chamber. Sulfur compounds were reduced in anodic chamber:

$$SO_4^{2-} + 8H^+ + 8e^- \rightarrow S^{2-} + 4H_2O \quad (14)$$

Reoxidization of S^{2-} occurred in the cathodic chamber:

$$S^{2-} + 2O_2 \rightarrow S/SO_4^{2-} + 8e^- \quad (15)$$

After nutrient removal and recovery process (Fig. 1), the self-generated electric field stimulated transfer of cation ions from anodic chamber (i.e. H^+, NH_4^+, K^+, Na^+, Ca^{2+}, Mg^{2+}) and anions from cathodic chamber (OH^-, SO_4^{2-}, PO_4^{3-}, NO_3^-, NO_2^-, Cl^-) to the middle chamber. As a result, NH_4^+-N could be recovered in the middle chamber rather than employing ammonia stripping and acid adsorption processes, thereby reducing energy demand and saving operational cost. PO_4^{3-}-P recovery also took place in the middle chamber with recovery efficiency of 37%. PO_4^{3-}-P as substrate for microbial growth was also removed in the anodic chamber, while no precipitation was detected in the cathodic chamber due to the migration of NH_4^+. Finally, this system showed excellent performance in removing 97-99% of urea, COD, SO_4^{2-} and PO_4^{3-}, and recovering 37-60% of total nitrogen, PO_4^{3-}, SO_4^{2-} and total salts.

2.3. Removal of emerging pollutants

The increasing consumption and usage of different types of emerging pollutants (i.e. antibiotics, pesticides, etc.) leads to residues of the pollutants presenting in aqueous environment (i.e., wastewater, rivers, groundwater), which deteriorates ecological balance and human health. Therefore, emerging pollutants need to be eliminated from wastewater before discharging into ecosystem. In MFC with bioanode, some emerging pollutants could act as electron donors in the presence of other carbon sources (i.e., glucose, acetate), which donate electrons to exoelectrogenic bacteria. The exoelectrogenic bacteria and some functional microbes for degradation of pollutants in anodic biofilm could oxidize emerging pollutants and generate electricity. The applied voltage in MEC with biocathode could enhance the electron transfer from anode to the biocathode, which accelerates degradation of pollutants by functional microorganisms on the biocathode.

2.3.1. Antibiotics removal

Generally, there are two pathways for antibiotics removal in BESs, including anodic-anaerobic biodegradation (AAB) and cathodic-electrochemical reduction (CER). Antibiotics are removed in the anodic chamber via AAB in BESs containing a biotic anode and an abiotic cathode. Microbes in the anodic chamber (antibiotic-degrading bacteria and other microorganisms (i.e. anaerobic microbes)) involve degradation and metabolization of antibiotics through reducing antibiotics' potential resistance to enable biodegradation and metabolization process, degrading metabolites as well as secreting degradation enzymes. External electrical current in BES could induce the direct or indirect transformation of electrons to the microbial cells, which stimulates microbial metabolism and enhances antibiotics degradation and mineralization. Antibiotics removal in MEC occurred in the cathodic chamber can be explained by the CER method, one is direct electrochemical reduction, by which emerging pollutants accepting electrons from the cathode can be directly eliminated, and another one is the associated overpotential reduction by the microbes

on the cathode as biocatalysts for biodegradation of antibiotics [9, 47-49]. This also significantly reduces antibiotic resistance genes (ARGs) production.

Sulfamethoxazole (SMX) degradation in MFC mainly occurred on anode. There are several different pathways for SMX degradation when an anode comprises anaerobic microorganisms or electroactive biofilm (EABF) consisting of electrochemically active microorganisms (Fig. 3). It was discovered that the MFC with added SMX (initial concentration of 20 mg/L) could remove more than 98% of SMX in the anode within 48 h of reaction [48, 50]. In the dual chamber MFC with anodic EABF, SMX affected energy metabolism and microbial activity through three mechanisms. The first was increasing the abundance of electrogenes (*Rhodopseudomonas*, *Geobacter*, and *Aquamicrobium*) responsible for energy generation, but eliminating some competitive species (*Alcaligenes* and *Nitrosomonas*) which utilize organic carbon or nitrogen for their growth or reproduction. For the second, it means stimulating generation of more EPS, i.e. redox proteins as electron shuttles or electroactive enzymes, to resist the toxicity of SMX and enhance reduction and oxidation reaction by altering redox system with anodic EABFs for power generation. It should be noted that SMX as an inhibitor limits bacterial reproduction, leading to less energy required for microbial growth and release of electrons for energy output.

Consequently, the MFC with anodic EABFs enhanced energy output by up to 15 times (reaching 1398.6 mW/m^2) and theoretically harvested 417 MW·h electricity for a plant treating 100,000 m^3 wastewater per day [50]. Norfloxacin (NFX) could be removed by MFC (65.5-48.4% at an initial concentration of 4-128 mg/L) using a high degree of acclimatization and high tolerance of anodic electrogenic microbes to high NFX concentration. Maximum power density reached up to 800 mV/m^2. Moreover, ARG generated was also reduced (10^5 copies/mL) compared to conventional wastewater treatment plants (generally 10^6-10^8 copies/mL). Nevertheless, it should pay attention to the adverse effects of higher NFC concentration (> 128 mg/L) on membrane

permeability of some exoelectrogenic bacteria. It not only inhibits the direct electron transfer through cell membranes from microorganisms to anode, but also increases internal resistance of MFCs [51].

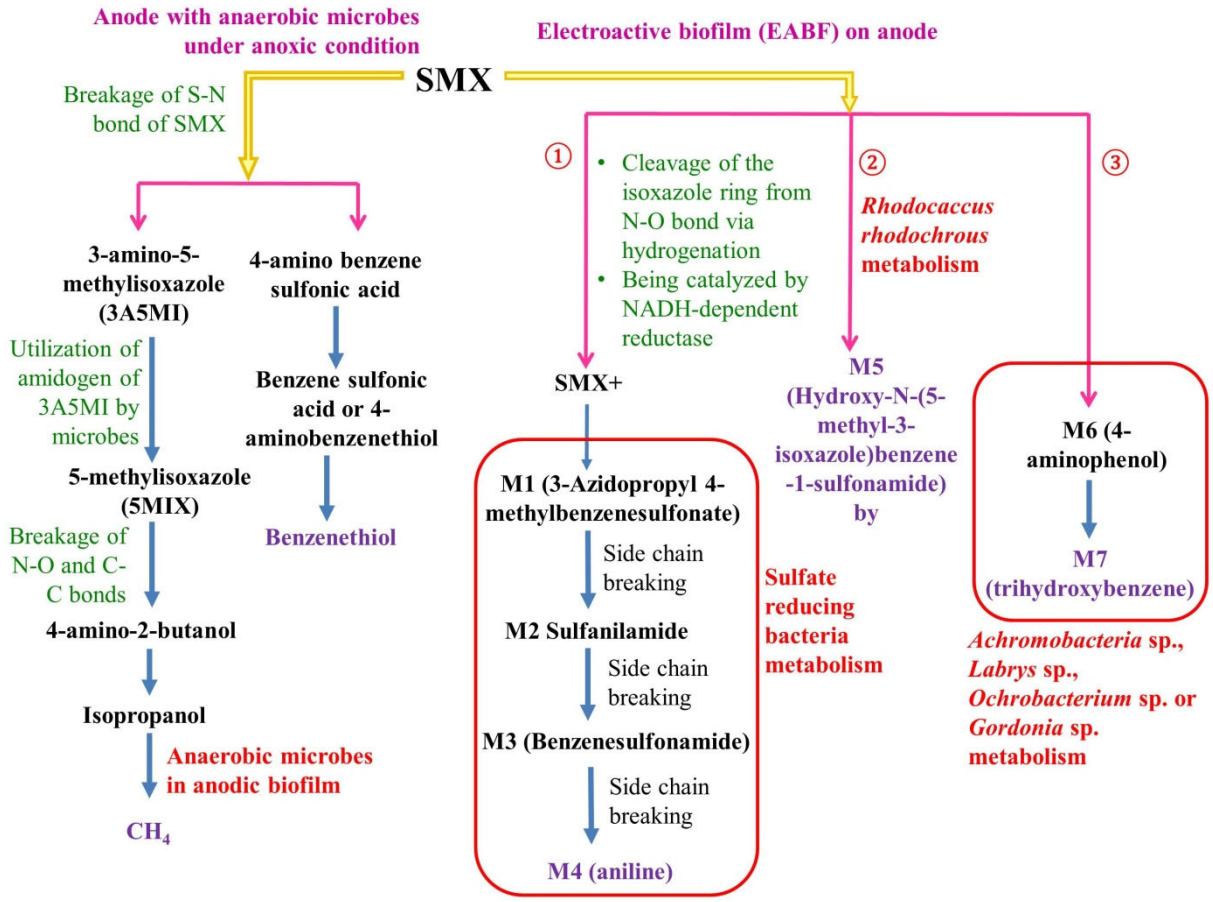

Fig. 3. Sulfamethoxazole (SMX) degradation pathways in dual chamber MFC based on information from Wang et al. [48] and Wu et al. [50]

In MEC, SMX degradation was not as high as that in MFC via different removal pathways (Fig. 4). At the applied voltage of 0.6 V, the increased SMX concentration and consistent electrical stimulation accelerated bioelectrochemical reactions. This led to better SMX degradation at higher initial SMX concentrations (removal of 77.6% at initial concentration of 10 mg /L vs 92.53% at 30 mg/L) when some SMX-resistant microorganisms (*Pseudomonas, Comamonas, Acinetobacter* and

Arthrobacter) were present on anode for SMX degradation. The removal of SMX could inhibit the production of ARGs (abundance of *intI1*, 1.23×10^2- 9.27×10^3 copies/g in MEC biofilms, 1.6×10^1-9.02×10^2 copies/mL in MEC effluents) compared to conventional wastewater treatment processes (> 1.75×10^9 copies/g for anaerobic digestion, 10^9-10^{11} copies/mL for WWTPs) [52]. Erythromycin (ERY) could be removed by 99% within 48 h in MEC. This was ascribed to the dominance of *Geobacter* (exoelectrogenic bacteria) in anodic biofilm (relative abundance of 77%) for generating electricity, and highly abundant *Acetoanaerobium* in biocathode (relative abundance of 11%) as exoelectrogen bacteria. This employs acetate as electron donor and carbon source for degrading pollutants [53].

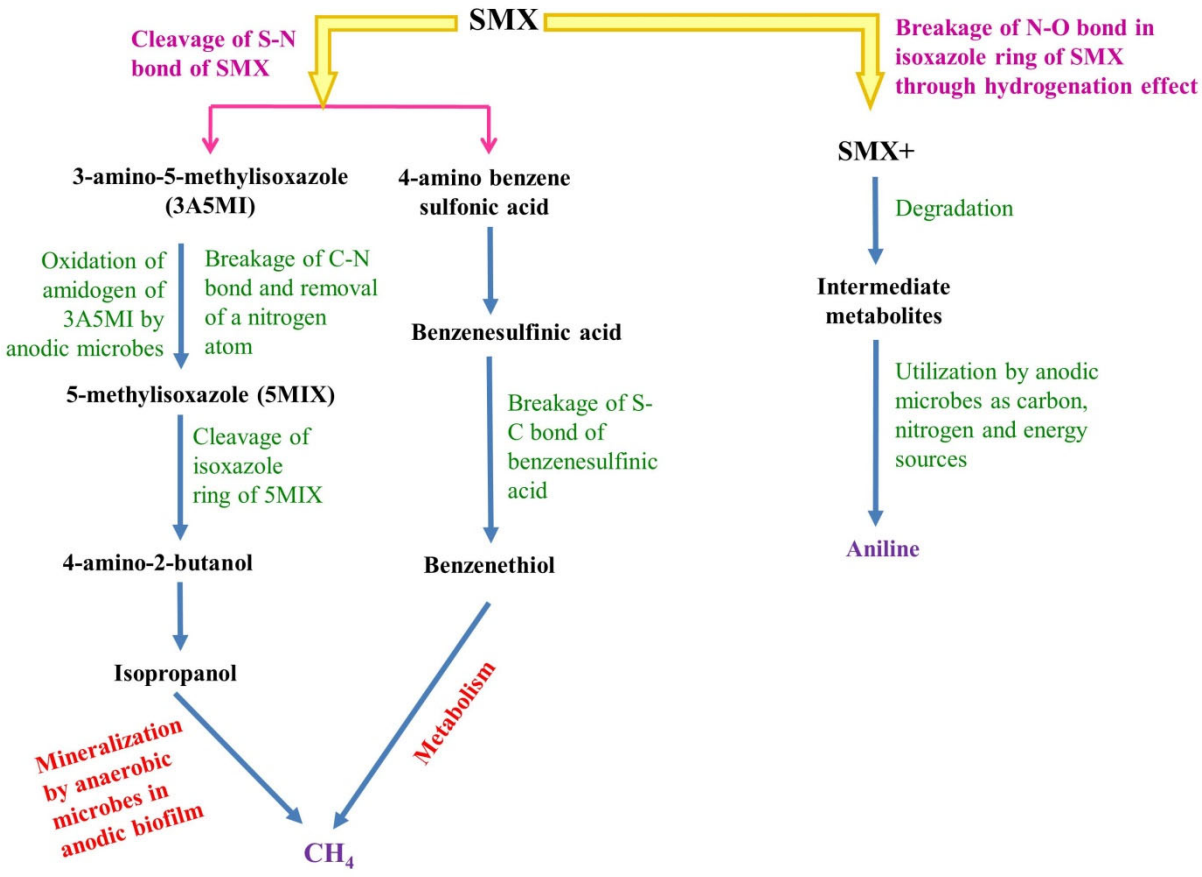

Fig. 4. SMX degradation in single chamber MEC based on information from Hua et al. [53]

382

383 **2.3.2. Removing other emerging pollutants**

384 Triclosan could be effectively removed in MFC (removal of 94% at initial concentration of 10
385 mg/L) via adsorption onto the anode with high surface area and porosity or biodegradation under
386 anoxic conditions by some species (i.e. *Geothrix, Corynebacterium, Sulfobacillus, GOUTA19,*
387 *Geobacter, Acidithiobacillus* and *Acinetobacter*). This contributes to the degradation of benzene-
388 related chemicals and dechlorination of chlorine-containing chemicals during TCS degradation
389 process [54, 55]. 17β-estradiol (E2) was removed in MEC by about 99.2% in 60 h due to the
390 dominant species *Bacillus, Lysinibacillus,* and *Aeromonas* contributing to E2 degradation. The
391 removal pathways included oxidization of E2 to hydroxylation products, ring opening oxidization
392 of the products by electrochemical reaction and microbial oxidase reaction to generate oxidative
393 products. There was also oxidation of oxidative products to macromolecules and organic
394 carboxylic acids with low molecular weight, and mineralization of organic carboxylic acids to CO_2
395 and H_2O [56]. MFC also removed a large amount of fipronil (94% at initial fipronil concentration
396 of 74 mg/L) in the presence of acetate as co-substrate in anodic chamber mainly via microbial
397 degradation in anode (metabolism of acetate) for generation of electrons and electricity by
398 electrogenic bacteria. It was followed by enhanced co-metabolic reaction efficiency of fipronil
399 degradation-related bacteria (*Azospirillum*, *Azoarcus*, *Chryseobacterium*) via accepting electrons.
400 Removals of various organic compounds were also high in the anodic chamber of MFC via
401 similar microbial catabolic pathways, i.e. 93% for 4-chloronitrobenzene (raw material or synthetic
402 intermediate in many industries), 84% for sulfanilamide (antibiotic and pharmaceutical
403 intermediate), 74% for fluoroglycofen (herbicide), and 65% for azoxystrobin (fungicide) [57].
404 MFC showed around 70% of sodium dodecyl sulphate (SDS) removal even at a high SDS
405 concentration of 40 mg/L by anodic biofilm containing some species (*Acinetobacter*,

406 *Pseudomonas*, *Citrobacter*, *Treponema,* etc.) able to degrade complex and refractory organics
407 through desulphurization, dehydrogenation, biotransformation and degradation. However, SDS did
408 endanger the formation of exoelectrogenic biofilm on the anode, which compromised power
409 performance of MFC by 66% and reduced maximum power density (12.7 W/m^2, 2.65-fold lower)
410 compared to the control MFC without SDS [58].

411 When treating azo dye wastewater (Sunset Yellow (SSY)), the mixed consortia in MFC after
412 acclimation could enhance their dye tolerance and increase decolorization ability (93% removal of
413 Sunset Yellow FCF, 96.6% removal of Allura Red, 91.41% removal of Tartrazine at initial
414 concentration of 100 mg/L). The presence of dye decoloring and exoelectrogenic bacteria
415 (*Klebsiella*, *Citrobacter*, *Enterococcus faecalis*, *Lactococcus garvieae*, *Proteus mirabilis*,
416 *Lactobacillus lactis*, and *Escherichia Shigella*) proved to be favorable for degrading intermediates
417 after breakage of azo bonds in azo dyes [59]. When using membrane-free electrolysis cell (MFEC)
418 with biocathode for azo dye treatment, the cathode fed with glucose as co-substrate generated
419 electrons via microbial respiration. The charge transfer resistance significantly reduced due to no
420 membrane being present. Thus, electrons were directly used for azo bond cleavage (breaking of
421 the chromophoric groups) to decolorize the Congo red dye (around 90% within 24 h at voltages of
422 0.3-0.9 V). MFEC also enabled CH_4 production by: firstly, directly utilizing electrons provided by
423 the cathode; and secondly, hydrogenophilic methanogenesis employing H_2 generated from the
424 cathode [60].

425 As sulfate reducing bacteria (SRB) can function as a biocatalyst involving microbial
426 extracellular electron transfer between microbes and electrodes, the enrichment of SRB on
427 electrodes (bioanode in MFC, biocathode in MEC) prompts the removal of some pollutants (i.e.,
428 chlorophenols, nitrobenzene, azo dye as electron acceptor) in the presence of sulfate. Additionally,
429 the presence of sulfur-oxidizing bacteria (SOB) on electrode (bioanode in MFC, biocathode in

MEC) for oxidation of sulfide releases electrons, which can be used to degrade pollutants (Fig. 5). At initial 4-CP concentration of 100 mg/L, MFC removed up to 40% of 4-chlorophenol (4-CP) with maximum power generation of 253.5 mW/m^2 (current density, 712.0 mA/m^2) after inoculating the anode with anaerobic sludge (containing sodium lactate and sodium sulfate) enriched with SRB [61]. Initially, acetate and propionate (electron donors) obtained by fermentation of lactase were oxidized to CO_2 in anodic biofilm where electrons transferred to the anode using SRB. Then sulfate (electron acceptor) was reduced to sulfide (electron donor) at the top of anodic biofilm (Eq. (16)), which maintained SRB growth. Sulfide was oxidized to sulfur via abiotic oxidation on the anode to generate electrons (Eq. (17)).

$$SO_4^{2-} + 8e \rightarrow H_2S/HS^- \quad (16)$$

$$H_2S/HS^- \rightarrow S^0/SO_4^{2-} + 2e \quad (17)$$

After that, reduction of 4-CP (electron acceptor) to phenol occurred by accepting electrons from anode, followed by reduction to acetate and again oxidation of acetate to CO_2 in the anodic chamber. In MEC, the increased external voltage applied heightened 4-CP removal compared to the MFC. At an applied cell voltage of 0.4 V versus Ag/AgCl, around 43% of 4-CP was removed in the anodic chamber. H_2O_2 was also produced in MEC (13.3 $g/L \cdot m^2$ after 6 h operation) via two-electron ORR at the cathode at pH 7:

$$3CO_2 + 10H^+ + 10e^- \rightarrow CH_2CHOHCOO^- + 3H_2O \ (E^0 = -0.34 \text{ V vs. normal hydrogen electrode (NHE)}) \quad (18)$$

$$10H^+ + 5O_2 + 10e^- \rightarrow 5H_2O_2 \ (E^0 = +0.26 \text{ V vs. NHE}) \quad (19)$$

This was made possible by higher cathode potential (around 260 mV vs. NHE) than anode potential (around -340 mV vs. NHE). Nevertheless, H_2O_2 may reduce to water when applying higher added voltage, competing with the two-electron ORR [61]:

$$H_2O_2 + 2H^+ + 2e^- \rightarrow 2H_2O \quad (20)$$

$H_2O_2 \rightarrow H_2O + 1/2O_2$ (21)

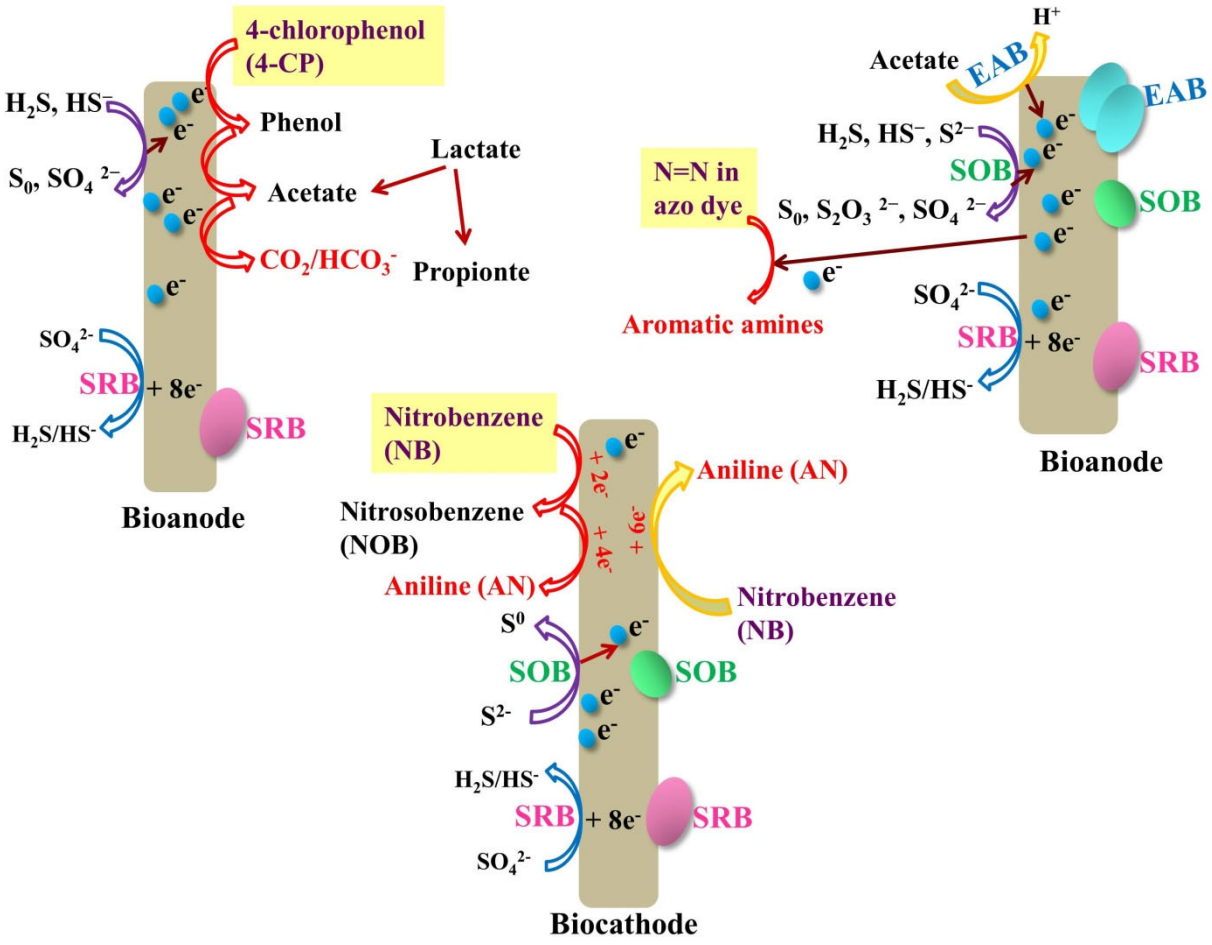

Fig. 5. Removal pathways for selected emerging pollutants in MFC with bioanode and MEC with biocathode based on information from Miran et al. [61], Luo et al. [62] and Dai et al. [63] Note: EAB, electrochemically active bacteria; SOB, sulfur-oxidizing bacteria; SRB, sulfate reducing bacteria

When treating wastewater containing nitrobenzene (NB, 50 mg/L) and sulfate (200 mg/L) by MEC with autotrophic SRB biocathode, NB removal efficiency reached 98%. Initially, NB was reduced to nitrosobenzene (NOB) using electricity. NOB was reduced to aniline (AN) using electrons from the cathode with *Wolinella* sp. present, which released nitrite reductase and this

467 involved the reduction of nitrite to ammonia. SRB (*Desulfovibrio* sp.) participated in the reduction
468 of sulfate to sulfide. During the process, electrons were provided by oxidation from sulfide to sulfur
469 by SOB (*Thioclava* sp. and *Halothiobacillus* sp.) [62]. During treatment of sulfide-containing azo
470 dye wastewater, the removal of Congo red dye (initial concentration of 200 mg/L) could reach
471 more than 88% by MFC with maximum power density of 24 W/m^2. This was accomplished in
472 three ways. Firstly, electrons were released through conversion of sulfide (HS^-, S^{2-}) to sulfur (S_0),
473 sulfate (SO_4^{2-}) and $S_2O_3^{2-}$ by SOB, which led to high sulfate concentration and deposition of
474 element sulfur on the electrode surface. Secondly, electrons and protons were generated by acetate
475 (co-substrate) due to the presence of electrochemically active bacteria (EAB), and thirdly, azo
476 bonds were cleaved in azo dye by accepting electrons to generate colorless products (i.e., aromatic
477 amines). Extracellular electron transport from microorganisms to electron acceptors (i.e. azo dyes,
478 anode) could be enhanced by cell lysis through biogenic sulfide reduction by SRB (genus
479 *Desulfovibrio*), which improved degradation of azo dyes [63].

480 MEC with EAB can also be a promising option for the treatment of dye wastewater treatment
481 through interaction between EAB and azo dye decolorization. EAB growth was selectively
482 enhanced by azo dye and extracellular decolorization of alizarin yellow R (AYR) realized by
483 extracellular electron transfer with EAB under electricity stimulation. This increased the removal
484 rate and limited toxicity of azo dye on EAB [64, 65]. Hou et al. [65] found that high decolorization
485 efficiency (around 90%) was obtained in a single-chamber MEC constructed with MoS_2-GO nickel
486 foam (NF) cathode at initial AYR concentration of 100 mg/L with co-substrate of NaAc and
487 glucose. Meanwhile, the electrons released by EAB in anode which were transferred to the cathode
488 stimulated H_2 generation.

489 Dual chamber MFC with electroactive biofilm carbon felt anodes could effectively remove 2-
490 chlorophenol (MFC-2-CP, initial concentration of 10 mg/L) and 2,4-dichlorophenol (MFC-2,4-

491 DCP, initial concentration of 10 mg/L) [66]. The anodic biofilm contained high biomass protein
492 level and many functional species consisted of exoelectrogens (i.e. *Geobacter*, *Pseudomonas*),
493 degrading bacteria (i.e. *Comamonas, Metagenome, Shinella, Dechlorosoma*) and multifunctional
494 electrogenic-degradative bacteria (i.e. *Acinetobacter*, *Azospirillum*). The first way of the removal
495 was biodegradation (95-97% for 2-CP, 84.5-88.7% for 2,4-CP) via dichlorination, hydroxylation,
496 and hydrogenation of 2-CP and 2-4-DCP into cyclohexanol with low toxicity, which encouraged
497 electricity generation by multifunctional microbial community in anodic biofilm:

498 2,4-DCP or 2-CP + $H^+ + e^- \rightarrow Cl^- +$ cyclohexanol (22)

499 The second was mineralization (74.7-80.5% for 2-CP, 58.8-78.4% for 2,4-CP) via the
500 production of long-chain hydrocarbons by ring opening reactions, followed by mineralization
501 hydrocarbons into CO_2 and H_2O:

502 Cyclohexanol → long-chain hydrocarbon → $CO_2 + H_2O + e^-$ (23)

503 Moreover, this process realized maximum power densities of 474.5 and 472.3 W/m^2 for 2-CP
504 and 2,4-CP, respectively [66].

505 As groundwater with low ion strength limited the removal of nitrate and perchlorate in BESs,
506 cathodic potential regulation was adopted using an electrochemical workstation with a three-
507 electrode system to limit the overpotential and enhance electron transfer in BESs to enhance
508 removals of nitrate and perchlorate. The application of negative potential shortened suppression
509 duration for perchlorate induced by nitrate (i.e. 55.6% of total reaction time at cathode potential of
510 -800 mV (vs SHE) vs 64.3% of total reaction time without potential regulation) and ameliorated
511 the inhibition effect of nitrate on perchlorate removal. At cathodic potential of -200 mV vs SHE,
512 the reduction rates of nitrate and perchlorate increased by 53.74% and 38.04%, respectively,
513 compared to MFC without potential control. Removals of nitrate and perchlorate were attributed
514 to both the cathode as electron donor and autotrophic bacteria, i.e. phyla *Proteobacteria,*

515 *Chloroflex, Ignavibacteriae,* classes *Betaproteobacteria* and *Alphaproteobacteria*) accepting
516 electrons for denitrifying and reducing the pollutants [67].
517
518 **2.4. Heavy metal removal**
519 Heavy metal in wastewater poses threats to the ecosystem and has adverse impacts (i.e., cancer
520 disease, liver and kidney damage, etc.) on different organisms. Hence, it needs to remove heavy
521 metal from wastewater to obtain clean water. This can be achieved by BES in three mechanisms.
522 The first is direct redox reaction (DRO) which is achieved by reducing metals to elemental deposits
523 or lower oxidation states through accepting electrons from cathode and/or cathodic biofilm (Table
524 1). The second is indirect byproduct precipitation (IBP) through precipitating metals with
525 byproducts of cathodic reduction reaction, i.e. OH^-, H_2O_2. Involved here is a single chamber MFC
526 with air cathode (Eqs. (24)-(27)) and cathodic hydrogen generation in MEC (Eqs. (28) and (29)):
527 $$O_2 + 2H_2O + 4e^- = 4OH^- \quad (24)$$
528 $$Me^{a+} + aH_2O \rightarrow Me(OH)_a\downarrow + aH^+ \quad (25)$$
529 $$Me^{4+} + 4H_2O \rightarrow Me(OH)_4\downarrow + 4H^+ \quad (26)$$
530 $$Me^{b+} + bOH^- \rightarrow Me(OH)_b\downarrow \quad (27)$$
531 $$2H_2O + 2e^- \rightarrow 2OH^- + H_2 \quad (28)$$
532 $$Me^{c+} + cOH^- \rightarrow Me(OH)_c\downarrow \quad (29)$$
533 The third is biological removal through intracellular/extracellular microbial respiration,
534 biological reduction, bioaccumulation and biosorption by anodic or cathodic biofilm. It should be
535 noted that precipitates in IBP may deposit on electrodes, ion exchange membrane, or other areas
536 of the cathode chamber. Removing metals through DRO and IBP requires further recovery
537 approaches, in other words manual scarping or acid dissolution after metal removal via DRO,
538 settling by gravity and collecting following metal removal via IBP. It has been reported that

539 excellent removal efficiencies above 95% were reported in more than 60% of studies. Meanwhile
540 other studies confirmed the removals of greater than 50% when metal concentrations ranging from
541 0.01-0.1 g/L as reported by above 50% in some research [38, 69-71].

542 **Table 1.** Heavy metal removal mainly via direct redox reaction (DRO) and biological removal*

Systems	**Metal removal with abiotic cathode in MFC (recovery)**	**Metal removal with abiotic cathode in MEC with external power supply (recovery)**	**Metal removal with biocathode in MFC (conversion)**	**Metal removal with biocathode in MEC (conversion)**
Conditions	Reduction potential of heavy metals at the cathode > oxidation potential of anode at the anode	Reduction potential of heavy metals at the cathode < oxidation potential of anode at the anode	Reduction potential of heavy metals at the cathode > oxidation potential of anode at the anode	Reduction potential of heavy metals at the cathode < oxidation potential of anode at the anode
Mechanisms	• Electrons generated through oxidation of organic substances at the anode • Direct reduction on the cathode surface, which is a spontaneous process (DRO) • Generation of net positive cell voltage	• Electrons generated through oxidation of organic substances at the anode • Electrons flowing from the anode to cathode driven by the external power supply and partial energy generated by BES • Direct reduction on the cathode surface (DRO)	• Electrons generated through oxidation of organic substances at the anode • Metals adsorbed into biofilm of the cathode from catholyte, which are reducing by specialized microorganisms via microbial respiration (DRO and biological removal)	• Electrons generated through oxidation of organic substances at the anode • Electrons flowing into the cathode driven by external power supply • Metal ions adsorbed onto the cathode and the biofilm on the cathode for reduction by microbes in biofilm (DRO and biological removal)
Examples of metals	$Ag^{+} \rightarrow Ag^{0}$ $Fe^{3+} \rightarrow Fe^{2+}$ $Cu^{2+} \rightarrow Cu^{0}$ $Se^{4+} \rightarrow Se^{0}$ $Hg^{2+} \rightarrow Hg^{0}$ $V^{5+} \rightarrow V^{4+}$	$Ni^{2+} \rightarrow Ni^{0}$ $Pb^{2+} \rightarrow Pb^{0}$ $Cd^{2+} \rightarrow Cd^{0}$ $U^{6+} \rightarrow U^{4+}$ $Co^{3+} \rightarrow Co^{0}$ $Zn^{2+} \rightarrow Zn^{0}$	$Cu^{2+} \rightarrow Cu^{0}$ $Se^{4+} \rightarrow Se^{0}$ $Hg^{2+} \rightarrow Hg^{0}$ $V^{5+} \rightarrow V^{4+}$ $Au^{3+} \rightarrow Au^{0}$ $Cr^{6+} \rightarrow Cr^{3+}$	$Cr^{6+} \rightarrow Cr^{3+}$ $U^{6+} \rightarrow U^{4+}$ $Ni^{2+} \rightarrow Ni^{0}$ $Cd^{2+} \rightarrow Cd^{0}$ $Co^{3+} \rightarrow Co^{0}$ $Zn^{2+} \rightarrow Zn^{0}$

	$Au^{3+} \rightarrow Au^{0}$	$Co^{3+} \rightarrow Co^{2+}$
	$Cr^{6+} \rightarrow Cr^{3+}$	
	$Co^{3+} \rightarrow Co^{2+}$	

*References: Guo et al. [38]; Kuma et al. [68]; Wang and He [69]

Removal of Cr(VI) in membrane-less dual chamber BESs was realized through initial bioelectrochemical Cr(VI) reduction by exoelectrogens on the cathode (Eq. (30)), and subsequent Cr(III) precipitation with phosphorus, which generate Cr-phosphorus precipitates and/or complexes on the cathode at neutral pH:

$Cr_2O_7^{2-} + 14H^+ + 6e^- \rightarrow Cr_2O_3 + 4H_2O + 6H^+ \rightarrow 2Cr^{3+} + 7H_2O$ ($E^0 = 1.33$ V) (30)

These were further removed from bulk sludge in BESs. Apart from this, MEC performed better in removing Cr(VI) and first-order Cr(VI) reduction rate constant (66.2% and 0.103/d, respectively) due to the external power supply compared to MFC (56.7% and less than 0.072/d, respectively) [72]. Moreover, Cu(II) was used as electron-shuttle mediators to enhance the removal of Cr(VI). The overpotential of cathode waned and the active energy barrier declined owing to the presence of Cu(II) in MFC, resulting in higher charge transport. Thus, Cu(II) improved the electron transfer from anode to cathode, which accelerated the indirect utilization of electrons generated by the anode for Cr(VI) reduction in the cathodic chamber as shown in Eqs. (30)-(33) and Cr(VI) reduction rate:

$Cu^{2+} + 2e^- \rightarrow Cu$ ($E^0 = 0.337$ V) (31)

or $2Cu^{2+} + H_2O + 2e^- \rightarrow Cu_2O + 2H^+$ ($E^0 = 0.207$ V) (32)

$2Cu_2O + 2H^+ + 2e^- \rightarrow 2Cu + 2H_2O$ ($E^0 = 0.059$ V)) (33)

As a result, $Cr(OH)_3$ and a little Cu were deposited on the cathode. At high levels of Cu(II) (50 mg/L), power density of 1235.53 mW/m^2 and Cr(VI) reduction rate of 1.191 $g/m^3 \cdot h$ were significantly higher (1.4 times and 1.17 times, respectively) than that without Cu(II) [73].

Electrochemical reduction in dual chamber BESs could successfully recovery sliver (above 80% during 48 h of operation) from the sliver(I) dithiosulfate $[Ag(S_2O_3)_2]^{3-}$ complex which was frequently detected in waster fixer solution from photographic processing waste. During the

operational stage, catholyte pH increased over time caused by: 1) cathodic reduction which decreased concentration of $[Ag(S_2O_3)_2]^{3-}$ but increased $[S_2O_3]^{2-}$; and 2) limited transportation of H^+ from anodic chamber to the cathodic chamber by other competitive cations (i.e. Na^+, K^+). This led to dominance of spontaneously electrochemical reaction converting $[Ag(S_2O_3)_2]^{3-}$ (electron acceptor) to metallic Ag^0 on the cathode surface [74]:

Anodic chamber:

$$CH_3COO^- + 4H_2O \rightarrow 2HCO_3^- + 9H^+ + 8e^- \ (E^0 = -0.289 \text{ V vs SHE}) \quad (34)$$

Cathodic chamber:

$$O_2 + 4H^+ + 4e^- \rightarrow 2H_2O \text{ (inoculation stage)} \ (E^0 = +1.229 \text{ V vs SHE}) \quad (35)$$

$$[Ag(S_2O_3)_2]^{3-} + e^- \rightarrow Ag^0 + 2S_2O_3^{2-} \text{ (operational period)} \ (E^0 = +0.016 \text{ V vs SHE}) \quad (36)$$

To overcome the problems induced by pH imbalance in two-chamber MFC (excess caustic in the catholyte and acidification in the anolyte), a loop of catholyte effluent feeding to bioanode in MFC with air cathode was developed by Song et al. [75]. This system could *in-situ* use caustic in the cathodes and neutralized acid generated in the anodes to recover metals. When feeding synthetic wastewater simulating printed circuit boards (PrCBs) processing wastewater at low organic loading of 200 mg/L, the cathodic chamber eliminated around 91% of Su, Fe and Cu, along with 68% of total COD removal. In the meantime approximately 8% of these metals were removed by the bioanodic chamber. Subsequently, more metals were deposited on the cathode (Sn(IV), Fe(III), Cu(0), and Cu(II)) than those on the anode. This reduced the adverse effects of the loop feeding design on the exoelectrogens on the anode. Besides, microorganisms in anodic biofilm were well acclimatized to the catholyte effluent containing metals, as demonstrated by the increased abundance of *Rhodopseudomonas* and *Geobacter* and the emergence of *Pseudomonas*, *Comamonas*, *Aeromonas* and *Azospira* in the microbial community on the anodes.

590 Electrodes enriched with SRB or EAB also act as biocatalyst and can enhance metal removal
591 in BESs. MEC with sulfate-reducer enriched biocathode was developed using two efficient SRB
592 strains (*Enterococcus avium* (BY7) and *Citrobacter freundii* (SR10)), which simultaneously
593 reduced sulfate and antimony (Sb) via sulfide metal precipitation and catalyzed hydrogen
594 generation. Although the metabolic activity of SRB strains abated under sudden adverse conditions
595 (Sb addition), a specified adaptation period helped to stabilize their activity. This improved sulfate
596 reduction and conversion of Sb(V) to Sb(III) as precipitation of Sb_2S_3 (conversion efficiency, up
597 to 70.1% with BY7 and up to 89.2% with SR10). The maximum total removal efficiencies of Sb
598 were 88.2% with BY7 and 96.3% with SR10 at sulfate reduction rates of 92.3 and 98.4 $g/m^3 \cdot d$,
599 respectively. However, hydrogen production rate declined after adding Sb (average 1.25-1.36
600 $m^3H_2/(m^3 \cdot d)$ vs 0.89-0.98 $m^3H_2/(m^3 \cdot d)$). This was ascribed to the adaptation to adverse conditions
601 and bioprecipitation of Sb reducing the electron transfer rate [76].
602 In single-chamber MECs with four EAB (*Citrobacter* sp. JY3, *Pseudomonas* sp. X3,
603 *Pseudomonas delhiensis* X5, *Ochrobactrum anthropic* X7) which can use HCO_3^- as carbon source
604 in BESs, various amounts of EPS with different compositions were released by these EAB to
605 strategically adapt to stressful conditions induced by the changes in initial Cd(II) and circuit
606 current. Compared to the bioanode, the biocathode was more favorable for Cd(II) recovery due to
607 the creation of anaerobic conditions which enhanced EAB activities and limited the consumption
608 of electrons by O_2. The high initial acetate level (5.0 g/L) changed the cathodic potential so that it
609 was more negative, which moderated the Cd(II) inhibition and enabled the removal of Cd(II) at a
610 wider range of initial Cd(II) concentration. Consequently, various Cd(II) removals (2.57–7.35
611 mg/L/h) and H_2 production (0–0.0011 $m^3/m^3 \cdot h$) were obtained at initial Cd(II) concentration of
612 20-150 mg/L and initial acetate concentration of 1.0-5.0 g/L due to the robustness of EAB [77].

3. Thermochemical conversion of biowastes and applications of the products

Biowastes are the wastes from animal, plants and human beings, for instance municipal solid waste, forestry and agricultural wastes, animal manures, food wastes, sewage sludge, etc. They contain certain amounts of energy, i.e. 10.73 MJ/kg for mustard stalk, 15.77 MJ/kg for olive refuse, 16.2 MJ/kg for peach bagasse, 17.97 MJ/kg for tobacco leaf, 22.00 MJ/kg for olive pits, etc. Consequently, they are ideal for generating biofuels/bio-energy through thermochemical conversion, in order to reduce dependence on conventional fossil fuel and greenhouse gas (GHG) emissions. Fig. 6 summarizes thermochemcial technologies for biowastes conversion and application of value-added products. Biowastes can be converted to various types of valuable products through pyrolysis: i) biochar (20-50%) as the main product, bio-oil (20-40%), syngas (10-25%) and some liquids (acetone, methanol, acetic acid) via slow pyrolysis (400-900 °C, residence time of minutes to days); ii) bio-oil as major products (60-75%) via fast pyrolysis (450-850 °C, residence time of 5-30 s); and iii) bio-oil (25-75%) and syngas (50-60%) as dominant products via flash pyrolysis (>1000 °C, residence time < 1-2 s) [16-18]. Biochar obtained by pyrolysis can be applied to wastewater treatment for removing heavy metals via surface complexation, ion exchange, cation-π electron, precipitation, etc., or used as adsorbent to remove organic micropollutants like 2, 4-Dichlorophenol, 2, 3, 4-Trichlorophenol, Bisphenol A, Carbamazepine, Androsterone, Estrone, 17a-Ethinylestradiol via pore-filling, hydrophobic interaction and electrostatic attraction [18, 22]. Bio-oil can be catalytically upgraded into petroleum-like biodiesel (surrogate fuel) or used as fuel to generate electricity in anion exchange membrane fuel cells. Besides, the syngas (especially CO and H_2 as dominant components) can be upgraded into diesel-like fuel or burned as fuel gas [18].

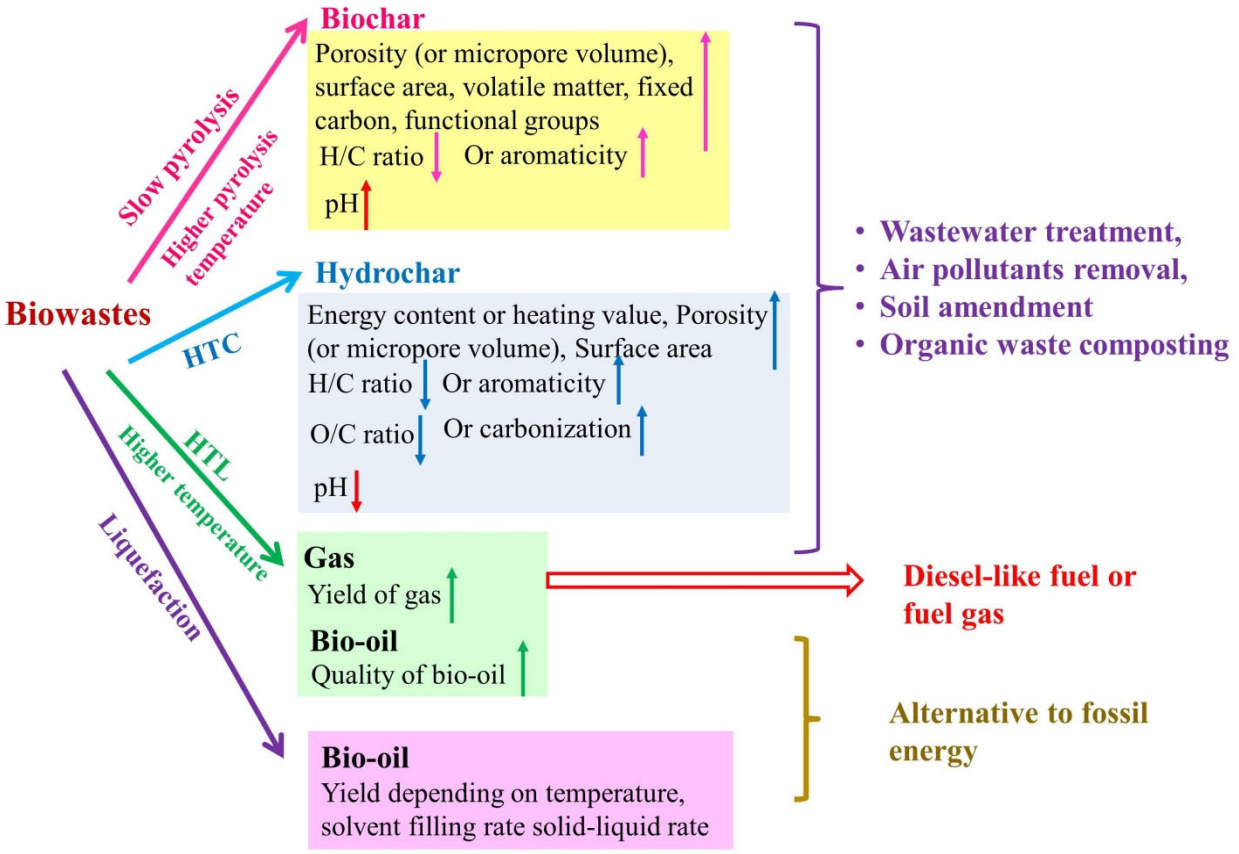

Fig. 6. Thermochemcial technologies for biowastes conversion and application of value-added products

It was found that slow pyrolysis temperature and types of biowastes affected biochar properties and their effects on soil amendment. For example, five different feedstocks (pine saw dust (SD), rice husk (RH), food waste (FW), poultry litter (PL) and paper sludge (PS)) were used for biochar preparation at four different pyrolysis temperatures (350, 450, 550 and 650 °C) [78]. Some important findings were specified as follows:

1) When pyrolysis temperature increased the pH of biochar also rose, i.e. increase in pH of both PL and PS from 6.2 to 10.3 in biochar. Thus, PS and PL biochars obtained at 550 and 650 °C could be used for acid neutralization in soil due to their pH buffer capacity.

2) The cation exchange value declined at higher pyrolysis temperature owing to loss of the organic functional group on biochar surface, aromatic C oxidation and formation of carboxyl groups. Hence, SD, PL and PS biochars at lower temperature (350 °C) were better for retention of soil nutrient.

3) The number of pores and pore size also increased at higher temperature, especially for SD and RS biochars. Moreover, BET surface area of all biochars increased, especially SD and RH biochars with higher surface area (431.91-443.79 m^2/g and 248.99-280.97 m^2/g). Thus, SD and RH biochar prepared at 550 and 650 °C favored water retention in the soil and the adsorption of pollutants.

4) The highest fixed carbon values were detected in SD (average 55.31%), RH (average 48.47%) and FW biochar (average 58.85%). The higher pyrolysis temperature increased the degree of aromaticity (decline in atomic ratio of hydrogen-oxygen (H/C)) but reduced polarity (decline in atomic ratio of oxygen-carbon (O/C)). Hence, RH and SD biochars obtained at higher pyrolysis temperature 550 and 650 °C (low O/C ratios, 0.1-0.26) were the most stable (half-life > 1000 years) among all biochars and could be applied for carbon sequestration into soil.

Gasification process at temperatures of 700-900 °C transforms biowastes to liquid and gaseous fuels as the dominant products used for transportation, and syngas employed in gas turbine. Torrefaction at low temperature of 200-300 °C under oxygen-free condition (mild pyrolysis) generates high-grade solid fuel from biowastes for power plant or boiler application. Hydrothermal liquefaction (temperature of 280-370 °C, pressure of 10-25 MPa) as high-pressure hydrolysis converts biowastes to high-quality bio-oil [16-18].

672 **3.1. Sewage sludge**

673 Sewage sludge can be converted into bio-oil, biochar and gas (H_2, CO and other light gases)
674 via pyrolysis which is a favored sludge management approach. Slow pyrolysis is divided into
675 carbonization and torrefaction. Carbonization mainly generates biochar, while torrefaction
676 increase heating value and C/H ratio of sewage sludge and eliminate NO_x, SO_x and other
677 pollutants. The porosity and surface morphology of biochar were increased by slow pyrolysis. pH
678 of biochar was higher than the raw sludge through the release of alkali salts, dehydration of sludge
679 feedstock and damage of organic acids and carbonates [79]. Fast pyrolysis can transform sewage
680 sludge to bio-oil consisting of hydrocarbons (aromatic and aliphatic ones), organic acids, and
681 carbonyl compounds with high molecular weight, aromatic and aliphatic compounds, nitrogenous
682 compounds, sulfur compounds and other compounds (i.e., phenols, ketones, etc.). The high initial
683 water content in sewage sludge (high humidity > 95% of water) and decomposition of volatile
684 matter during fast pyrolysis reduce heating value and induce the presence of oxygenated
685 compounds in the bio-oil. Thus, compared to petroleum derived heavy fuel oil (average 40 MJ/kg),
686 the bio-oil obtained via fast pyrolysis of sewage sludge possesses higher moisture content and
687 lower HHV (average 30 MJ/kg) [28].

688 There are two alternative options to enhance both the quality and quantity of products during
689 pyrolysis; one is co-pyrolysis and another is catalytic pyrolysis. Co-pyrolysis of sewage sludge
690 with other biowates (i.e. saw dust, rice straw, etc.) not only can enhance deoxygenation and
691 increase heating value of bio-oil and improve quality of bio-oil, but also increase heating value
692 and specific surface area of biochar. Catalytic pyrolysis with additives or catalysts (i.e. Al_2O_3,
693 CaO, Fe_2O_3, TiO_2, ZnO) can upgrade bio-oil with stable storage value by increasing carbon and

694 hydrogen yield, reducing oxygen and water content, increasing HHV of bio-oil, decreasing
695 viscosity and minimizing pollutants [28].

696 Hydrothermal carbonization (HTC) and hydrothermal liquefaction (HTL) have also been
697 employed to prepare valuable products (i.e., hydrochar, bio-oil) from sewage sludge. HTC process
698 improves energy content of hydrochar by transforming low energy density chemical bonds (i.e., –
699 C-O and –C-H) into high energy chemical bonds (-Aryl). As the amount of aromatic carbon
700 increases after HTC treatment, the aromaticity of carbon in hydrochar increases [30]. HTC
701 increased the porosity and surface area of hydrochar produced compared to the sludge feedstock,
702 while decreasing H/C and O/C ratios that enhanced aromaticity and carbonization. However, pH
703 of hydrochar decreased compared to sludge feedstock as acidic functional groups generated via
704 hydrolysis reaction. The heavy metals enriched in hydrochar that are in bioavailable fraction could
705 be converted into stable fraction. Thus, these metals presented minimal or no environmental risk
706 for field application [79]. Since the aromatic carbon content increases in the hydrochar after the
707 HTC process, hydrochar possesses high soil carbon sequestration potential. Moreover, the
708 hydrochar can also be used as land fertilizer due to the residual N (ammonia obtained by
709 deamination) and P (extractable phosphate) [30]. Although recent works tried to improve
710 hydrochar yield by adding some chemical catalysts during HTC process, the hydrochar could not
711 be used as cleaner fuel with better heating value (HV). This was ascribed to that hydrochar
712 obtained after adding NaCl or employing ammonia-treated Fenton sewage sludge as feedstock
713 demonstrated declined carbon composition, HV and H/C ratio [80].

714 HTL treatment can generate bio-oil having HHV of 30-40 MJ/kg from sewage sludge. Higher
715 temperature improves the quality of bio-oil and yield of gas. Solvents (i.e. methanol, ethanol)
716 during HTL process stimulate the generation of esters, and improve the yield and quality of bio-

717 oil. Sludge pretreatment (i.e., subcritical water, fatty alcohol polyoxyethyleneether, ultrasonic,
718 etc.) can improve hydrocarbons, HHV, energy recovery, aromaticity and/or polarity of bio-oil
719 obtained after HTL. Through regulating products from HTL by catalysts (i.e. $CuSO_4$, $NiMo/Al_2O_3$,
720 $Cu(NO_3)_2$), bio-oil (i.e. esters, amides)) and gas generation can be enhanced, while limiting coke
721 formation [30].

722 It needs to pay more attention to polycyclic aromatic hydrocarbons (PAH) as PAH in sewage
723 sludge is the toxic and recalcitrant organic pollutants. The increased reaction temperature (220-
724 360 °C) and diminished solid-liquid ratio (sewage sludge-pure water ratio, 0.05-0.20) reduced the
725 total content of PAHs in biochar. The total content of PAHs was the lowest at relatively lower
726 reaction temperature of 300 °C, solid-liquid ratio of 0.1 g/mL and shorter reaction time of 30 min
727 in the range of 0-60 min. When reaction temperature or time increased, more PAHs transferred
728 into bio-oil (89% of PAH in bio-oil). Any further treatment or utilization of bio-oil was inhibited
729 by high toxic equivalent quantity (TEQ) values (6.1–8.6 mg/kg) and total content of PAHs in bio-
730 oil (55.0–106.6 mg/kg). Thus the HTL process needs to be improved to reduce the formation of
731 PAHs [81].

732

733 **3.2. Agricultural wastes, food waste and municipal solid waste (MSW)**

734 The biochars generated from different feedstocks are used for wastewater treatment (i.e., COD
735 and polyphenol from cork wastewater, fluoxetine (FLX), common dyes (i.e. methylene blue,
736 methyl violet and rhodamine B), herbicide from agricultural surface water, nutrient from human
737 urine, as well as air pollutants removal (i.e., naphthalene ($C_{10}H_8$), benzene) (Table 2). Agricultural
738 wastes can be transformed to syngas via gasification and biochar via carbonization or pyrolysis.
739 Syngas is mainly used to generate heat and power in the combined heat and power (CHP) plants

740 or via co-firing of the gas produced from large-scale power plants, or generation of electricity by
741 energy conversion device (gas reciprocating engines, gas turbines).

742 **Table 2.** Conversion of biowastes to value-added products through thermochemical technologies and applications of the products
743

Types of biowastes[a]	Thermochemical technologies	Products and properties[b]	Applications[c]	References
Agricultural residues				
CCS	Gasification	• High conversion of CCS to syngas (composition, 19.53% H_2, 16.32% CO and 3.42% CH_4) • Being highly capable in generating bioenergy • High energy efficiency (32.8%) caused by the high calorific value of synthesis gas and low energy requirement of gasification process	➢ Syngas used for electricity generation in a gas engine as fuel ➢ H_2 as a valuable and clean alternative to fossil fuel that feeds low-temperature fuel cells and allows electric energy conversion	[75, 82]
CPH	Gasification in a commercial 115 kW_{th} biomass gasifier	• Generation of syngas (20.3-23.8% of CO, 12.5-16.2% of H_2, 2.3-3.2% of CH_4) • Maximum calorific value of 6.13 MJ/Nm^3, CCE of 82% and cold gas efficiency of 68% obtained at the optimum equivalence ratio and moisture content (0.25 and 5%, respectively)	N.A.	[83]
Coconut powder	N.A.	Commercial biochar (CPAC) • Porosity structure with the • High BET surface area (1952 m^2/g), • Micropore volume (1.76 cm^3/g) • Mesopores volume (1.57 cm^3/g)	➢ High removal of COD (up to 98%) and polyphenol (100%) during cork wastewater treatment via adsorption after flocculation (flocculant, $FeSO_4 \cdot 7H_2O$) ➢ Maintaining textural properties and adsorption capability of the biochar by MW-assisted regeneration process for five	[84]

			cycles of regeneration and adsorption	
OPMF	Carbonization at 600 °C for 30 min and subsequent activation with steam for 30 min	Biochar • High surface area of 494 m^2/g	➢ COD reduced from 395 to 122 mg/L after six consecutive cycles when treating biologically treated palm oil mill final discharge, which met the river water limit of 50-150 mg/L of COD	[85]
Palm kernel shell	Microwave pyrolysis and steam activation at a fast heating rate of 20 °C/min for 65 min	Biochar • 83 wt% yield of biochar with high surface area (419 m^2/g) • Low moisture content (~5 wt%) • A microporous structure	➢ Adsorption of herbicide from agricultural surface water (2,4-D) at 11 mg 2,4-D/g biochar	[86]
Rice bran	Pyrolysis at 500 °C for 2 h (heating rate of less than 5 °C/min) with nitrogen flow at 3 L/min autoclave post-treatment	Biochar • High surface area 120 m^2/g, • Low H/C ratio 0.04	➢ Removal of FLX from aqueous media (92.6% at initial FLX concentration of 50 mg/L) ➢ The adsorption process fitted well with the pseudo-2nd order kinetic and Freundlich isotherm, implying the electrostatic attractions dominated the adsorption of FLX onto the biochar surface	[87]
Waste wood	Pyrolysis at 500 °C	• Waste wood-based biochar • Surface area, 412.25 nm^2 • Porous and amorphous structure • Being made of graphite and amorphous carbon • uneven mixing or agglomeration	➢ Reduce VOCs (naphthalene ($C_{10}H_8$), dichloroethane ($C_2H_4C_{l2}$) and normal octane (C_8H_{18})) emissions from asphalt when heating at a high temperature (> 100 ºC) by 50%	[88]
Soft wood pellet	Pyrolysis at 700 °C	• High surface area of 162 m^2/g	➢ Adsorption of benzene (2.9 mg/g) via partition and physisorption process, which was related to surface area of biochar	[89]
Rice husk	Pyrolysis at 550 °C	• N.A.	➢ Adsorption of MEK (43 mg/g) associated with favorable nature	[89]

			of feedstock, surface properties and composition of biochar	
PKS, EFB	slow pyrolysis (50 mL/min N_2 at 500 °C)	• High biofuel quality and high HHV of PKS-derived biochar and EFB-derived biochar (26.18–27.50 MJ/kg) • Relatively high biochar yield of 35.14-37.07% • Low average (the apparent activation energy) E_a of 169.36-205.70 kJ/mol • Low moisture content of 1.03-2.26%	➢ High biofuel potential	[90]
Mixture of wood waste	Being treated by $MgCl_2$ solution followed by pyrolysis at 600 °C under a N_2 gas environment	Mg-biochar • Irregular morphology of crystals on the surface • Mg crystals on the surface including periclase (MgO) and magnesium hydroxide ($Mg(OH)_2$)	Removal of nutrient from human urine ➢ Maximum capacity for nutrient removal of 47.5 mgN/g and 116.4 mgP/g ➢ 70% removal of phosphate by precipitation on Mg-biochar ($Mg_3(PO_4)_2$, $MgHPO_4$, $Mg(H_2PO_4)_2$) as Mg^{2+} released from MgO on the biochar reacted with phosphate ➢ 30% removal of phosphate by adsorption through chemical bonding and electrostatic interaction between ≡Mg-OH and PO_4^{3-} as well as between biochar surface with positive charge and phosphate anions (HPO_4^{2-} and $H_2PO_4^-$ in the pretreated urine at pH range of 8.4-8.9)	[91]

			➢ Nutrient removal from wastewater containing low ratio of ammonium to phosphate (i.e. swine wastewater) and anaerobic digestion supernatant of activated sludge	
Food wastes				
COSCG	Pyrolysis under optimal pyrolytic conditions (CO_2 as atmospheric gas, 110-min pyrolytic time)	• The prepared Co-biochar catalyst contained metallic Co and surface wrinkled carbon layers. • Syngas including H_2 (~ 1.6 mol% in non-isothermal pyrolysis for 50 min) and CO (~ 4.7 mol% in isothermal pyrolysis for 60 min) was generated during thermochemical process of COSCG	➢ Co-biochar showed catalytic capability in removing PNP (reaction kinetic in the range of 0.04-0.12/s)	[92]
Mixture of discarded vegetables and fruits	Slow pyrolysis at high temperature of 600 °C (heating rate of 5 °C/min)	Biochar • Higher carbon content (60.7 wt% vs 51.7% at 300 °C), • Higher HHV (23 MJ/kg vs 20.6 MJ/kg at 300 °C), • higher surface area (4.9 m^2/g vs 0.85 m^2/g at 300 °C), • Higher aromatic-vinylic content (66.3% vs 50.1% at 300 °C), • Higher alkaline pH (11.2 vs 7.9 at 300 °C), • Higher electrical conductivity (8.7 mS/s vs 4.3 mS/s at 300 °C) Bio-oil • Higher HHV 32.4 MJ/kg vs 23.5 MJ/kg at 300 °C	Applications of biochar ➢ Adsorbent, ➢ Catalyst, ➢ Support, ➢ Soil amendment agent or precursor for activated carbon Applications of bio-oil ➢ Hexadecanoic acid and octadecanoic acid for generation of soaps, detergents and cosmetic products ➢ Phenols for production of ➢ plastics, cosmetics and disinfectants ➢ Ricinoleic acid for pigment and textile finishing	[15]

		• Main components, acids, alcohols and phenols Gases • Higher HHV (8.4 MJ/Nm^3 vs 1.1 MJ/kg at 300 °C) due to higher concentrations of H_2 and CH_4		
Food waste	Slow pyrolysis at 600 °C for 60 min (heating rate of 5 °C/min), followed by KOH activation at 800 °C and 90 min (activation time) with nitrogen flow rate of 150 mL/min	FW-AC-KOH • BET surface area, 1760 m^2/g • Total pore volume, 0.94 cm3/g • Average pore size, 3.7 nm • Biochar yield, 48.8%	➢ Complete removal of methylene blue, methyl violet from aqueous solution during 1-2 h of contact time ➢ 91% removal of rhodamine B	[93]
GCW	Thermal treatment of Mg^{2+} loaded GCW in a pyrolyzer (heating rate of 10 °C/min) using N_2 gas as carrier gas (200 mL/min) from room temperature to 500 °C	Mg-biochar • Higher surface area (36.4 m^2/g vs 0.2 m^2/g for the control biochar) • Higher pore volume (0.11 vs 1.38 × 10^{-4} cm^3/g for the control biochar) • Higher average pore size (116.5 Å vs 27.8 Å for the control biochar)	Adsorption of phosphate ➢ Phosphate adsorption capacity (63.5 mg P/g biochar) by Langmuir model ➢ Maximum phosphate adsorption of 56 mg P/g biochar via electrostatic adsorption Fertilizer ➢ Production of magnesium phosphate crystal, $Mg_3(PO_4)_2$ through forming covalent bonds between phosphates and Mg^{2+} of the Mg-biochar in aqueous solution (≡ MgO + H_2O → ≡ $MgOH^+$ + OH)	[94]

Mixed biowastes				
LW containing sawdust, animal forage, manure, *etc.*	CO_2-assisted one-stage pyrolysis (650 °C for 1 h) with flow rate of CO_2 at 200 mL/min	Biochar • High alkaline contents Ca (10.51 wt%), Mg (2.30 wt%), K (1.98 wt%), and Al (0.60 wt%) • Surface area: 16.356 m^2/g, • Total pore Volume: 0.037 cm^3/g, • Mean pore diameter: 9.13 nm	➢ Enhanced syngas generation by the biochar as a catalyst during pyrolysis of LW ➢ Proportional relationship between the catalytic capability of biochar and the amount of catalyst loading	[95]
CM + agricultural waste (CS, GM)	Integrated thermochemical conversion process CM hydrochar (HC 2hr CM) prepared by mild hydrothermal carbonization (220 °C for 2 h); Mixing HC 2hr CM with CS (CS + HC 2hr CM) or GM (GM + HC 2hr CM), followed by pyrolysis at 600 °C for 1 h	• Heterogeneous biochar (CM + GM or CM + CS) with enriched bioavailable nutrients (P, K, and Mg) compared to manure hydrochar and agricultural wastes • Bio-oil mainly consisting of ketones, phenols, alkanes, alkenes	➢ Soil amendment ➢ Surrogate petroleum fuel after upgrading the biofuel generated	[96]
Mixture of urea and wood residue	Preparing mixture at urea: wood residue ratio of 100:1, followed by calcining at a ramping	N-doped biochar • Highest graphitic N (N% w/w) formation compared to low ratios as more N was doped onto carbon structure of biochar at higher initial urea concentration (12.1%N (w/w)	➢ PMS activator with considerably high catalytic activity for organic pollutants removal via nonradical pathway (i.e. complete removal of AO7)	[97]

	rate of 10 °C/min to temperature of 800 °C and maintaining the temperature for 2 h under oxygen-free condition, and finally drying in an oven	at ratio of 100:1 vs 8.0-8.2%N (w/w) at ratios of 25:1 and 50:1) • Highest specific surface area compared to other ratios (588 m^2/g at ratio of 100:1 vs 407 and 502 m^2/g at ratios of 25:1 and 50:1) • Rough external surface with wrinkles and creases (defective sites) and smooth internal surface • Formation of phenolic groups at defective sites and declined lactonic groups at reactive sites for N attachment	

[a] CCS, coffee cut-stems; CM, cow manure; COSCG, cobalt (Co)-loaded lignin-rich spent coffee grounds; CPH, cocoa pod husk; CS, corn stover; EFB, empty fruit bunch; GCW, ground coffee waste; GM, grape marc; LW, livestock waste; OPMF, oil palm mesocarp fiber; PKS, palm kernel shell; CCE, carbon conversion efficiency which represents the percentage of total moles of carbon-bearing components in produced gas (PG (CO, CO_2 and CH_4) to the carbon composition present in CPH

[b] CPAC, coconut powder activated carbon; FW-AC-KOH, potassium hydroxide (KOH) activation of food waste biochar; HHV, higher heating value

[C] AO7, acid orange 7; FLX, fluoxetine; MEK, methyl ethyl keton; PMS, peroxymonosulfate; PNP, p-nitrophenol; VOC, volatile organic compounds; 2,4-D, 2,4-dichlorophenoxyacetic

After thermochemical conversion at temperature of 300 °C for 2 h, polar groups (i.e. alcohol, esters, ketones, aldehydes, carboxylic, ether and phenols) appeared in both orange (*Citrus sinensis*) peels (OP) and albedo (OA) derived biochar. Compared to OP biochar, OA biochar possessed more carbon, inorganic elements, slightly higher surface area (352.5 m^2/g for OP biochar and 356.3 m^2/g for OA biochar) and smaller porous surface (micropore volume, 0.148 (OP) and 0.145 m^3/g (OA); total pore volume, 0.217 (OP) and 0.215 m^3/g (OA); pore diameter, 2.132 (OP) and 2.138 nm (OA)). In contrast, OP derived biochar had a smooth surface. Therefore, OP derived biochar could be used for adsorbing pollutants from water and soil. OA derived biochar was adopted for enhancing soil nutritional value, fertilizer production and GHG emissions and carbon sequestration in soils [98].

Compared to biochar properties at lower pyrolysis temperatures (200 and 300 °C), the biochar obtained after pyrolysis of leaf waste at 400 °C had higher volatile matter and fixed carbon, lower H/C ratio and higher pH of biochar (10.23) due to the formation of alkaline species, higher BET surface area, pore volume and micropore volume [99]. Biochar can be used for the removal of H_2S (84.2%) from gas generated during anaerobic digestion process by: firstly, formation of a water film on biochar surface owing to its lower hydrophilicity resulting from lower H/C ratio; secondly, adsorption of H_2S on biochar surface, forming dissolution with water film (Eq. (37)); and thirdly, dissociating the adsorbed H_2S molecule in water film (Eq. (38)) and reacting with adsorbed trace oxygen, which generated elemental sulfur inside pores (Eqs. (39) and (40)):

$$H_2S_{(gas)} \rightarrow H_2S_{(ads)} \rightarrow H_2S_{(ads\text{-}liq)} \quad (37)$$

$$H_2S_{(ads\text{-}liq)} + OH^- \rightarrow HS^-_{(ads)} + H_2O) \quad (38)$$

$$HS^-_{(ads)} + O_2 \rightarrow S^0 \quad (39)$$

$$HS^-_{(ads)} + O_2 + H_2O \rightarrow SO_4^{2-} \quad (40)$$

774

775 Tea waste biochar (TB) prepared by pyrolysis at 500 °C (heating rate of 7 °C/min for time
776 duration of 2 h) possessed high porosity and high surface area (312.43 m^2/g), and indicated high
777 metal immobilization ability. When treating sediment with 10% TB, Cd was reduced by 67.7% in
778 the exchangeable fraction. During the meso-microcosm study, it was discovered that the uptake of
779 Cd in mollusk tissue, and root and shoot of water hyacinth declined by 75-87%. This might be
780 attributed to excellent properties of TB favorable for Cd sorption, including large amounts of
781 micro-meso, meso- and macro-pores as well as high surface area on TB surface, aromatic structure
782 on TB surface, and more oxygen functional groups on TB which offered surface ligand binding
783 site. Additionally, negative surface charge of TB (electron-rich surface) also prompts adsorption
784 of Cd ions at low pH (< 8.5) through π^+-π electron donor-acceptor interactions. Moreover, ion
785 exchange between Cd ions and cations on TB surfaces (Ca^{2+}, Mg^{2+}) also contributed to Cd removal
786 [100]. Engineered tea-waste biochar (high surface area 576 m^2/g) prepared by pyrolysis at 700 °C
787 using steam activation (TWBC-SA) reached maximum caffeine adsorption capacity of 15.4 mg/g
788 at pH 3.5. Caffeine could be adsorbed onto TWBC-SA via: i) chemisorption as the dominant
789 removal mechanism involving nucleophilic reaction between nitrogen atoms of the five-membered
790 ring of caffeine molecule and the carbonyl groups on the biochar surface under acidic condition;
791 ii) formation of covalent bonds and electrostatic attraction; and iii) physisorption on the biochar
792 surface via π-π and hydrogen bonding between hydroxyl groups of biochar surface and
793 heterocyclic group of caffeine molecule [101].

794 The biochar-bentonite composite was obtained by mixing bentonite suspension with MSW
795 (1:5 ratio (w/w)) and subsequent pyrolysis. The maximum adsorption capacity of the composite
796 was higher (190 mg/g, 40% higher) than that of the pristine biochar. It was ascribed to the

797 generation of more active sites, diffusion of ciprofloxacin (CPX) molecules into the interlayer
798 space of the clay mineral via hydrogen bonding between oxygen-containing functional group of
799 CPX and free hydroxyl groups on the composite. Also responsible was enhanced electrostatic
800 interactions between the functional groups of the composite and CPX molecules after modification
801 [102]. It was found that relatively higher pyrolysis temperature favored the generation of biochar
802 with better characteristics prepared from MSW containing wood-based products (i.e. molded wood
803 pallets, sawmill cut ends, plywood, particle boards, etc.). Compared to pyrolysis temperature of
804 400 °C (74.3-85.3%, 0.10-0.14 cm^3/g and 215.0-359.84 m^2/g), biochar produced after pyrolysis at
805 higher temperature of 600 °C possessed more fixed carbon (81.4-94.0%), higher micropore volume
806 (0.15-0.21 cm^3/g) and surface area (298.4-509.3 m^2/g) without soluble PAH. Although some
807 biochars contained high levels of trace metals (i.e., mercury (Hg) from painted wood derived
808 biochar, arsenic (As) from treated wood derived biochar), most trace metals could be effectively
809 eliminated by acid washing, especially acetic acid favorable for dissolving minerals. It also
810 required more attention being paid to the management of some potential pollutants (chlorine,
811 nitrogen and sulfur) in the biochar [103].
812
813 **3.3. Animal manure**
814 Thermochemical liquefaction of pig or cattle manure generally uses ethanol as a solvent since
815 ethanol provides active hydrogen to decompose biomass, improve the stability of liquefaction
816 intermediates and limit the formation of hardly decomposed compounds. Operation conditions and
817 types of manure feedstocks affected the generation of bio-oil. During thermochemical liquefaction
818 of pig manure, the relatively lower liquefaction temperature of 220 °C prompted maximum yield
819 of bio-oil (31.4% of liquefied products) than those at higher liquefaction temperatures of 260 and

300 °C. This was due to the crude protein and lipid in pig manure raw material. However, during liquefaction of cattle manure, fragmentation of polymers into liquid oil-rich phase was enhanced at higher temperature (300 °C) with maximum bio-oil (OCM) relative yield of around 32% and absolute yield of 23 kg/kg compared to that at lower temperature (180, 220 and 260 °C). Furthermore the yield of bio-oil was affected by solid-liquid rate (determined by the quantity of the manure sample and the volume of the liquid solvent) and solvent filling rate (the rate of the volume of the liquid solvent divided by the fixed volume of the reactor). When using pig manure as feedstock, the yield of bio-oil declined at higher solid-liquid rate (proportions in liquefied products, 35.56% at 5% vs 22.04% at 15%) due to the weak interaction between solvent molecules and biomass molecules. On the other hand, the production rate of bio-oil rapidly increased at higher solvent filling rate (10-15%). The obtained bio-oil had similar components from pig and cattle manures, including esters, long-chain hydrocarbons, ethanol and nitrogen compounds. The heating values of bio-oil derived from animal manure after thermochemical liquefaction were significantly higher than the manure feedstocks. The heating value of pig manure liquefied bio-oil (37.03 MJ/kg) was close to the heating value of gasoline (46 MJ/kg). Meanwhile the higher and lower heating values of cattle manure liquefied bio-oil (25.63-33.41 MJ/kg and 23.85-31.39 MJ/kg, respectively, vs 10.87 MJ/kg and 9.74 MJ/kg for cattle manure feedstock, respectively) strongly suggested their potential as alternative commercial fuels to fossil fuel energy [104, 105].

Zhou et al. [106] pointed out that compared to slow pyrolysis (400-600 °C), HTC was a more effective way to convert animal manure to hydrochar since the HTC process narrowed the weight loss temperature range for the animal manure. When employing the HTC process, the hydrochar properties were affected by the types and nature of feedstocks. The HHVs of different livestock and poultry manure increased after HTC, i.e. 15.18 MJ/kg of swine manure (SM) vs 16.14 MJ/kg

of SM hydrochar, 15.26 MJ/kg of dairy cattle manure (DCM) vs 18.43 MJ/kg of DCM hydrochar, 13.72 MJ/kg of beef cattle manure (BM) vs 15.77 MJ/kg of BM hydrochar, 12.77 MJ/kg of broiler litter (BL) vs 16.22 M/kg of BL hydrochar, and 14.27 MJ/kg of layer chicken litter (LL) to 18.05 MJ/kg of hydrochar. At 210 °C, energy yields were the highest for biochars of SM, BL and LL (65.5%, 56.9% and 64.4%, respectively). Animal manure derived biochar can be employed for generating syngas. The biocrude obtained from pyrolysis of DCM under CO_2 condition contained high levels of hetero-hydrocarbons and aromatic compounds, which were not suitable for liquid fuels in combustion engines. Hence, DCM derived biochar was employed to transform biocrude to syngas during DCM pyrolysis with CO_2 serving as a gaseous medium at ≤ 600 °C. CO formation was enhanced by gas phase homogeneous reactions between CO_2 and gas phase volatile compounds originating from DCM pyrolysis. The gas phase reactions and chemical bond damage of biocrude induced by alkaline metal(oxide)s (i.e., $CaCO_3$) in biochar as catalyst (3 g/L) significantly enhanced H_2 and CO formation (> 5-fold) compared to non-catalyst pyrolysis [107].

3.4. Other applications of biochars

During organic waste (i.e., pig manure, sawdust, beer vinasse, etc.) composting process, biochar addition can increase pile porosity and improve oxygen permeability (O_2 supply), which avoid anaerobic fermentation. It can also improve organic matter degradation, extend duration of thermophilic phase and increase composting temperature, which enhance compositing efficiency and humidification process. Biochar addition encourages N mineralization and N retention, which minimize the formation of large clumps. It is possible to mitigate N_2O emissions as the large amounts of aromatic compounds (C-O bond, C-H bond) in biochar contacted with NO_3^--N, which encourage the formation of π-π electron donor or acceptor interactions and further inhibit

866 denitrification. Adding biochar can reduce CH_4 emissions due to the formation of aerobic reaction,
867 survival and proliferation of methanotrophs caused by high pore volume and good pore structure
868 of biochar. Biochar also can reduce odor emissions since NH_4^+-N and NH_3 are adsorbed by pores
869 and surface acid groups of biochar, and furthermore enhance enzymatic activities and degradation
870 rate. Heavy metals are stabilized by surface and inner-sphere precipitation and complexation as
871 well as physical adsorption. Furthermore freely dissolved PAHs are reduced [20].
872 Biochar can be also used for adsorption of air pollutants (volatile organic compounds (VOCs))
873 via physical adsorption to carbonized fraction (Van der Waals interactions, π-π electron donor–
874 acceptor interactions, and pore-filling processes) and partitioning process involving partitioning
875 into organic phase or to noncarbonized organic matter faction [89, 108, 109]. Biochar can also be
876 used for GHG emissions (CO_2, NO_2, CH_4) and other gases (i.e. SO_2, H_2, H_2S, etc.). When adopting
877 constructed wetlands for wastewater treatment, biochar might improve nitrous oxide reductase
878 activity, adsorb NH_4^+-N and NO_3^--N to reduce N_2O emissions from nitrification or denitrification,
879 and inhibit the activity of microorganisms responsible for nitrification and mineralization, thereby
880 reducing N_2O emissions. The reduction of CO_2 emissions after adding biochar might be induced
881 by precipitating CO_2 as carbonate (biochar has high surface pH and high levels of alkaline metals),
882 adsorbing organic matter, reducing some abundant carbohydrate-mineralizing enzymes (i.e.
883 glucosidase, celloboisidase), and increasing plant growth for greater net exchange of CO_2 between
884 environment and CWs [21].
885 Biochar exerts positive effects on arid soils by: 1) enhancing water retention capacity since
886 biochar can retain water; 2) improving nutrient holding potential given that biochar can keep N-
887 nutrients/ fertilizers; 3) removing cations (heavy metals) from soil through carbon sorption; 4)
888 eliminating organics (i.e. hydrocarbons, pharmaceuticals) through adsorption due to its high

889 porosity, large surface area and surface functional groups; 5) increasing crop yields through
890 improving irrigation conditions and soil quality (increased N, P, K contents and solid organic
891 carbon) because biochar possesses some nutrients (N, P, K, Ca); and 6) stabilizing heavy metals.
892 This favors the increase in crop yield. It is worth noting that soil microorganisms are positively
893 affected by biochar addition through increasing water availability, improving aeration condition,
894 removing toxic compounds by sorption, neutralizing soil pH value, retaining nutrient in soil, and
895 offering shelters, nutrients and electron donors [17, 20].

896 As biochar possesses porous structure and large surface area, it can provide electroactive sites
897 to accumulate charges (Faradaic reaction), which in turn realizes high capacitance, i.e. capacitance
898 of 344 F/g and power density of 850 W/kg for argy warm wood-derived biochar, 346.1 F/g and
899 160 W/kg for *Cotonier strobili* Fibers-derived biochar, 168 F/g and 1500 W/kg for Fructose corn
900 syrup-derived biochar. For these reasons biochar can be used as electrode materials in
901 supercapacitors, which are energy storage materials and employed in electronic devices,
902 automobiles, air-craft or locomotive systems [18].

903

904 **3.5. Nutrient recovery**

905 Sewage sludge is enriched with phosphorus (total phosphorus, 13-122.09 g/kg) in three
906 different forms, including inorganic phosphorus, poly-phosphate and organic phosphorus. After
907 thermochemical treatment, phosphorus also exists in ash (aluminum calcium phosphate
908 ($Ca_9Al(PO_4)_7$), aluminum phosphate ($AlPO_4$), iron phosphate ($FePO_4$)), aqueous phase
909 (orthophosphate), and biochar/hydrochar (hydroxyapatite ($Ca_5(PO_4)_3OH$, octacalcium phosphate
910 ($Ca_8H_2(PO_4)_6 5H_2O$, $FePO_4$, $MgPO_4$, $Mg_2(PO_4)_3$, $AlPO_4$) [110]. Besides, animal manure and food
911 waste also contain high levels of phosphorus (total phosphorus up to 34.10 and 52.00 g/kg,

912 respectively) [111]. Thus, phosphorus recovery from sewage sludge, animal manure or food waste
913 by thermochemical technologies is a promising way to deal with finite sources of natural
914 phosphorus.

915 After HTC process, phosphorus is transformed into orthophosphate in liquid fraction,
916 insoluble precipitates in the hydrochar due to the reaction between metal elements (i.e. Ca, K, Mg)
917 in the feedstock (recovery > 90%) and phosphorus, as well as adsorption via affinity of Fe and Al
918 hydroxides with phosphorus [111]. Subsequently, phosphorus recovery can be conducted via wet-
919 chemical extraction process from ash and hydrochar. For example, inorganic acids (e.g.
920 hydrochloric acid (HCl), sulfuric acid (H_2SO_4), nitric acid (HNO_3), phosphoric acid (H_3PO_4))
921 dissolve alkali-metal oxides and induce phosphorus release. On the other hand, metals or
922 metalloids and metal-bound P are released in the presence of organic acids (e.g. oxalic acid
923 ($C_2H_6O_6$), citric acid ($C_6H_8O_7$), gluconic acid ($C_6H_{12}O_7$), formic acid (CH_2O_2), acetic acid
924 ($C_2H_4O_2$)) through chelating effects. Alkaline extraction (i.e. NaOH) can extract phosphorus from
925 ash and hydrochar as well as inhibit the dissolution of heavy metals. After coupling the wet-
926 extraction method and precipitation process with addition of precipitants (i.e. $CaCl_2$, $MgCl_2 \cdot 6H_2O$
927 and/or NH_4^+-rich wastewater or thermochemical process water, etc.), phosphorus can be
928 significantly recovered (close to 100% of phosphorus precipitation efficiency) as $AlPO_4$,
929 $Ca_3(PO_4)_2$, $FePO_4$, struvite, hydroxyapatite and other products (i.e. calcium phosphate,
930 chlorophosphate, etc.) [112].

931 Chemical reagents (i.e. CaO, acids, etc.) can be also directly added during thermochemical
932 conversion process to enhance nutrient recovery. The direct addition of CaO during hydrothermal
933 treatment process can induce the formation of hydroxyapatite (being abundant in nature P ores)
934 which is highly stable, easily productive and biocompatible and has high potential in enhancing

935 growth of plants [113, 114]. During the HTC process, the alkaline environment (pH up to 8.58)
936 induced by high HTC temperature (> 200 °C) prompted the conversion of organic phosphorus
937 (OP, polyphosphate) to inorganic phosphorus (IP, orthophosphate), and favored the enrichment of
938 apatite phosphorus (AP) in the hydrochars. Orthophosphate (PO_4^{3-}) reacted with Al^{3+}, Fe^{2+} and
939 Mg^{2+} from sludge feedstock to form $FePO_4$, $AlPO_4$ and $Mg(PO_4)_2$. After adding sufficient CaO
940 (loading ratio of 4%), some $Ca(OH_2)$ was formed, leading to an alkaline solution. Then PO_4^{3-} was
941 released from $FePO_4$, $AlPO_4$ and $Mg(PO_4)_2$:

942 $$Me(PO_4)_n + 3nOH^- \rightarrow Me(OH)_{3n}\downarrow + nPO_4^{3-} \text{ (M = Al, Fe, Mg)} \quad (41)$$

943 Some of the released PO_4^{3-} was used to form hydroxyapatite ($Ca_5(PO_4)_3OH$):

944 $$5Ca^{2+} + 3PO_4^{3-} + OH^- \rightarrow Ca_5(PO_4)_3OH\downarrow \quad (42)$$

945 Some organic phosphorus (pyrophosphate) was converted to $Ca_2P_2O_7{\cdot}2H_2O$. Thus, non-
946 apatite inorganic phosphorus (NAIP) was almost completely transformed into AP as
947 hydroxyapatite ($Ca_5(PO_4)_3OH$) and $Ca_2P_2O_7{\cdot}2H_2O$. This significantly increased apatite
948 phosphorus by 252% in hydrochars and P-availability by 233% compared with that in hydrochar
949 obtained via HTC without CaO addition [113]. Table 3 summarizes some typical thermochemical-
950 based nutrient recovery processes.

951 **Table 3.** Nutrient recovery through different thermochemical-based recovery processes

952

Feedstocks	Recovery processes[a]	Key findings[b]	Nitrogen and/or phosphorus recovery[c]	References
Anaerobically digested sewage sludge	Acidification of sludge slurry with nitric acid, followed by HTC at 180 °C for 2 h, phosphate leaching using citric acid, and finally forced struvite precipitation* at pH of 9.0 with NaOH	• Removal of phosphate from hydrochar by acid leaching process • Rapid formation of struvite using ammonia-rich liquid from HTC (107-291 mmol/L NH_4), pH adjustment and magnesium source	➢ Up to 82.5% of phosphate recovery	[115]
Anaerobically digested sewage sludge	HTC at 200 °C for 30 min, followed by addition of $MgCl_2$ in hydrolysate obtained, and pH adjustment	• Optimum nutrient recovery obtained at pH of 9 and Mg/P molar ratio of 1	➢ Up to 91.60% of PO_4-P recovery and 54.88% of NH_4^+-N recovery from the hydrolysate with MAP purity of 84.24%	[116]
Sewage sludge	Hydrothermal treatment at 200 °C, 220 °C or 240 °C for 0.5 h with addition of CaO, which combined with steam gasification at 900 °C and steam/hydrochar (or sludge) mass ratio of 2.4: 1	• More than 14 mg/g of phosphorus enriched in hydrochar after hydrothermal treatment • Significant removal of organic phosphorus from hydrochar by destruction and recovery of most inorganic phosphorus after hydrothermal treatment • Conversion of some of organic phosphorus to inorganic phosphorus during hydrothermal treatment at temperatures of 220-240 °C	➢ Up to 85% of total phosphorus recovery when hydrothermal treatment was operated 200 °C	[114]

		• Enhanced transformation of NAIP to AP at higher pH with CaO addition • Complete removal of OP and almost complete recovery of IP during gasification steam process		
Swine manure	TH at 120 or 170 °C for 1 h with addition of H_2SO_4 (0.1 M); HTC at 200 or 250 °C for 1 h with addition of H_2SO_4 (0.1 M)	• pH- and temperature-dependent phosphorus extraction and better phosphorus extraction under acidic conditions • Temperature-dependent nitrogen extraction • Enhanced phosphorus extraction in the presence of acid (H_2SO_4) compared to solutions of other organic acids (CH_3COOH or HCOOH) and NaOH solution • Maximum nitrogen (organic N plus NH_4^+-N) extraction obtained with H_2SO_4 after TH at 170 °C	➢ The highest phosphorus extraction (94%) and only 6% of phosphorus in hydrochar with H_2SO_4 after TH at 170 °C	[117]
Swine manure	Mixing with HCl + H_2O_2 and being treated by TH at 90-150 °C for 10-80 min	• Two periods for phosphorus solubilization and transformation during TH process, including initial increase in conversion of phosphorus to PO_4^{3-}-P in the processing water and subsequent decline in conversion over time • Enhanced nitrogen solubilization and transformation into NH_4^+-N at higher temperature and longer reaction time • High conversion of phosphorus and nitrogen obtained at relatively high temperature of 140 °C and short residence time of 30 min	➢ Almost 100% struvite crystallization efficiency from the supernatant at Mg^{2+}/PO_4^{3-} and pH of 9.11	[118]
Cattle manure	Acid-supported HTC at 190 °C for 12 h with 2% HCl	• More than 90% of phosphorus that was extracted in the form of PO_4-P in HCl solution	➢ Being close to 100% and 64% of phosphorus and	[119]

		• Existence of critical pH for release of TN and NH_4^+-N • More extracted nitrogen at higher acid concentration	nitrogen extraction, respectively	
Spent coffee grounds	HTC at 200 °C for 5 h, which generated HTC process water, followed by nanofiltration and finally chemical precipitation by adjusting pH to 9 with NaOH	• Converting around 83% of total phosphorus in feedstock into dissolved ortho-P after HTC • Concentrating inorganic nutrient (PO_4-P, Mg^{2+}) by nanofiltration, resulting in a high mass concentration factor 3.9 times • The molar ratios of Mg, NH_4^+-N and PO_4-P after nanofiltration rejection favorable for struvite precipitation	➢ High recovery of aqueous phosphorus at around 93% after simple pH adjustment ➢ About 75% of total phosphorus recovery from feedstock as pure struvite ($MgNH_4PO_4 \cdot 6H_2O$)	[120]

*Forced struvite precipitation, phosphate-rich hydrochar leachate was initially mixed with liquid from ammonia rich process (HTC process) to reach molar ratio of NH_4: PO_4 close to 1, and then mixed with $MgCl_2$ to have a stoichiometric relation of Mg: PO_4 to 1.3

[a] HTC, hydrothermal carbonization; TH, thermal hydrolysis

[b] AP, apatite phosphorus; IP, inorganic phosphorus; NAIP, non-apatite inorganic phosphorus; OP, organic phosphorus; TN, total nitrogen

[c] MAP, $MgNH_4PO_3 \cdot 6H_2O$

4. Future perspectives

Current studies have extended the applications of BES from nutrient removal/recovery to biogas upgrade, removing emerging pollutants and heavy metals from wastewater. BES-EMG can convert CO_2 captured by or dissolved into wastewater to CH_4. Emerging pollutants are effectively removed either by bioanode in MFC or biocathode in MEC due to the electrode enriched with special functional microbes which contribute to degradation of pollutants and enhanced electron transfer and generation. The addition of some metals (i.e., Cu(II)) can enhance the electron transfer as electron-shuttle mediators to enhance removal of the target metals (i.e., Cr(IV)). BES containing electrode rich in EAB or SRB also enhances heavy metal removal. Biowastes are converted to value-added products (including biochar/hydrochar, gas and bio-oil) through thermochemical processes. Furthermore, these products' properties are better than the feedstocks (i.e., enhanced porosity, surface area and heating value of biochar/hydrochar, increased bio-oil yield, etc.). Subsequently, products can be widely employed for environmental sustainability, such as wastewater treatment, soil amendment, surrogate fuel and fossil energy. However, more studies are required to enhance the functioning of these technologies and properties of products as follows:

1) In-depth studies should concentrate on more possible pathways for conversion of CO_2, H_2 and other gases to CH_4 by BES;
2) Removal of a wider range of emerging pollutants in BES are needed to be investigated deeply comprehensively;
3) More types of special functional microorganisms on electrodes should be explored and mechanisms about removing pollutants in the presence of these microbes must be clarified;
4) More advanced thermochemical technologies can be devised to simplify the operational process and enhance the properties of products;

5) Wider range of biowastes should be employed for making high value-added products;
6) More studies need to explore applications of products obtained from thermochemical technologies.

5. Conclusions

This review updated the studies published on the development and applications of BESs in the treatment of wastewater containing nutrient, emerging pollutants and heavy metals. Nitrogen is removed and recovered on anode and cathode, while phosphorus recovery is mainly accomplished via chemical precipitation on the cathode. The bioanode in MFC or biocathode in MEC enriched with EAB and/or SRB accelerates electron transfer and generation and further degradation of pollutants. Thermochemical technologies transform biowastes to value-added products (including biochar/hydrochar, gas and bio-oil) with better characteristics than feedstocks. Moreover, the products can be widely applied in wastewater treatment and soil amendment, as surrogate fuel and fossil energy for environmental sustainability. Some types of biowastes are also potential feedstocks for phosphorus recovery by thermochemical treatment. Future studies should concentrate on more types of special functional microbes on electrodes as well as preparation and applications of products obtained from thermochemical conversion of biowastes.

Acknowledgement

This research was supported by University of Technology Sydney, Australia (UTS, RIA NGO; UTS, 2021 SRS) and the Korea Institute of Energy Technology Evaluation and Planning (KETEP) and the Ministry of Trade, Industry & Energy (MOTIE), Republic of Korea (No. 20183020141270 and No. 20194110300040).

References

[1] Y. Duan, A. Pandey, Z. Zhang, M.K. Awasthi, S.K. Bhatia, M.J. Taherzadeh, Organic solid waste biorefinery: Sustainable strategy for emerging circular bioeconomy in China, Ind. Crops. Prod. 153 (2020) 112568. https://doi.org/10.1016/j.indcrop.2020.112568

[2] United Nation, The Sustainable Development Goals Report 2020. https://unstats.un.org/sdgs/report/2020/ (Assessed 19 November 2021)

[3] United Nation, The Sustainable Development Goals Report 2021. https://unstats.un.org/sdgs/report/2021/ (Assessed 19 November 2021)

[4] R. Gurjar, M. Behera, Treatment of Organic Fraction of Municipal Solid Waste in Bioelectrochemical Systems: A Review, Special Collection on Bioelectrochemical Systems: Excitement and Reality, J. Hazard. Toxic Radioact. Waste. 24 (2020) 04020018.

[5] T.M.W. Mak, X. Xiong, D.C.W. Tsang, I.K.M. Yu, C.S. Poon, Sustainable food waste management towards circular bioeconomy: Policy review, limitations and opportunities, Bioresource Technology 297 (2020) 122497. https://doi.org/10.1016/j.biortech.2019.122497

[6] S. Ilyas, R.R. Srivastava, H. Kim, S. Das, V.K. Singh, Circular bioeconomy and environmental benignness through microbial recycling of e-waste: A case study on copper and gold restoration, Waste Manage. 121 (2021)175-185.

[7] P. Sharma, V.K. Gaur, R. Sirohi, S. Varjani, S. Hyoun Kim, J.W.C. Wong, Sustainable processing of food waste for production of bio-based products for circular bioeconomy, Bioresour. Technol. 325 (2021) 124684. https://doi.org/10.1016/j.biortech.2021.124684

[8] S. Jung, J. Lee, Y.K. Park, E.E. Kwon, Bioelectrochemical systems for a circular bioeconomy, Bioresour. Technol. 300 (2020)122748. https://doi.org/10.1016/j.biortech.2020.122748

[9] A. Ahmad, M. Priyadarshani, S. Das, M.M. Ghangrekar, Role of bioelectrochemical systems for the remediation of emerging contaminants from wastewater: A review, J. Basic Microbiol. 2021 Sep 17. https://doi.org/10.1002/jobm.202100368

[10] A. Ceballos-Escalera, D. Molognoni, P. Bosch-Jimenez, M. Shahparasti, S. Bouchakour, A. Luna, A.Guisasola, E. Borràs, M.D. Pirriera, Bioelectrochemical systems for energy storage: A scaled-up power-to-gas approach, Appl. Energy 260 (2020) 114138. https://doi.org/10.1016/j.apenergy.2019.114138

[11] K. Chandrasekhar, G. Kumar, S.V. Mohan, A. Pandey, B.-H. Jeon, M. Jang, S.H. Kim, Microbial Electro-Remediation (MER) of hazardous waste in aid of sustainable energy generation and resource recovery, Environ. Technol. Innov. 19 (2020) 100997. https://doi.org/10.1016/j.eti.2020.100997

[12] R.R. Bora, R.E. Richardson, F. You, Resource recovery and waste-to-energy from wastewater sludge via thermochemical conversion technologies in support of circular economy: a comprehensive review. BMC Chem. Eng. 2, 8 (2020). https://doi.org/10.1186/s42480-020-00031-3

[13] Z. Fang, Y. Gao, N. Bolan, S.M. Shaheen, S. Xu, X. Wu, X. Xu, H. Hu, J. Lin, F. Zhang, J. Li, J. Rinklebe, H. Wang, Conversion of biological solid waste to graphene-containing biochar for water remediation: A critical review, Chem. Eng. J. 390 (2020) 124611. https://doi.org/10.1016/j.cej.2020.124611

[14] X.J. Lee, L.Y. Lee, S. Gan, S. Thangalazhy-Gopakumar, H.K. Ng, Biochar potential evaluation of palm oil wastes through slow pyrolysis: Thermochemical characterization and pyrolytic kinetic studies, Bioresour. Technol. 236 (2017) 155-163. https://doi.org/10.1016/j.biortech.2017.03.105

[15] B.R. Patra, S. Nanda, A.K. Dalai, V. Meda, Slow pyrolysis of agro-food wastes and physicochemical characterization of biofuel products, Chemosphere 285 (2021) 131431. https://doi.org/10.1016/j.chemosphere.2021.131431

[16] A.M. Elgarahy, A.Hammad, D.M. El-Sherif, M. Abouzid, M.S. Gaballah, K.Z. Elwakeel, Thermochemical conversion strategies of biomass to biofuels, techno-economic and bibliometric analysis: A conceptual review, J. Environ. Chem. Eng. 9 (2021) 106503. https://doi.org/10.1016/j.jece.2021.106503

[17] S. Elkhalifa, T. Al-Ansari, H.R. Mackey, G. McKay, Food waste to biochars through pyrolysis: A review, Resour. Conserv. Recycl. 144 (2019) 310–320. https://doi.org/10.1016/j.resconrec.2019.01.024

[18] S.Y. Foong, R.K. Liew, Y. Yang, Y.W. Cheng, P.N.Y. Yek, W.A.W. Mahari, X.Y. Lee, C.S. Han, D.-V. N. Vo, Q.V. Le, M. Aghbashlo, M. Tabatabaei, C. Sonne, W. Peng, S.S. Lam, Valorization of biomass waste to engineered activated biochar by microwave pyrolysis: Progress, challenges, and future directions, Chem. Eng. J. 389 (2020) 124401. https://doi.org/10.1016/j.cej.2020.124401.

[19] G. Jiang, D. Xu, B. Hao, L. Liu, S. Wang, Z. Wu, Thermochemical methods for the treatment of municipal sludge, J. Clean. Prod. 311 (2021) 127811. https://doi.org/10.1016/j.jclepro.2021.127811.

[20] X.X. Guo, H.T. Liu, J. Zhang, The role of biochar in organic waste composting and soil improvement: A review, Waste Manage. 102 (2020) 884-899. https://doi.org/10.1016/j.wasman.2019.12.003.

[21] F. Guo, J. Zhang, X. Yang, Q. He, L. Ao, Y. Chen, Impact of biochar on greenhouse gas emissions from constructed wetlands under various influent chemical oxygen demand to nitrogen ratios, Bioresour. Technol. 303 (2020) 122908. https://doi.org/10.1016/j.biortech.2020.122908.

[22] P. Regkouzas, E. Diamadopoulos, Adsorption of selected organic micro-pollutants on sewage sludge biochar, Chemosphere 224 (2019) 840-851. https://doi.org/10.1016/j.chemosphere.2019.02.165.

[23] A. Jain, Z. He, "NEW" resource recovery from wastewater using bioelectrochemical systems: Moving forward with functions, Front. Environ. Sci. Eng. 12, 12 (2018) 1. https://doi.org/10.1007/s11783-018-1052-9

[24] J. De Vrieze, J.B.A. Arends, K. Verbeeck, S. Gildemyn, K. Rabaey, Interfacing anaerobic digestion with (bio)electrochemical systems: Potentials and challenges, Water Res., 146 (2018) 244-255. https://doi.org/10.1016/j.watres.2018.08.045.

[25] V.G. Gude, Integrating bioelectrochemical systems for sustainable wastewater treatment. Clean Techn. Environ. Policy 20 (2018) 911–924. https://doi.org/10.1007/s10098-018-1536-0

[26] Md T. Noori, M.T. Vu, R.B. Ali, B. Min, Recent advances in cathode materials and configurations for upgrading methane in bioelectrochemical systems integrated with anaerobic digestion, Chem. Eng. J. 392 (2020) 123689. https://doi.org/10.1016/j.cej.2019.123689

[27] R.A.A. Meena, R.Y. Kannah, J. Sindhu, J. Ragavi, G. Kumar, M. Gunasekaran, J.R.Banu, Trends and resource recovery in biological wastewater treatment system, Bioresour. Technol. Rep. 7 (2019) 100235. https://doi.org/10.1016/j.biteb.2019.100235

[28] N. Gao, K. Kamran, C. Quan, P.T. Williams, Thermochemical conversion of sewage sludge: A critical review, Prog. Energy Combust. Sci. 79 (2020) 100843. https://doi.org/10.1016/j.pecs.2020.100843

[29] M. Hu, Z. Ye, H. Zhang, B. Chen, Z. Pan, J. Wang, Thermochemical conversion of sewage sludge for energy and resource recovery: technical challenges and prospects, Environ. Pollut. Bioavailab. 33(2021)145-163. https://doi.org/10.1080/26395940.2021.1947159

[30] X. Zhang, X. Li, R. Li, Y. Wu, Hydrothermal Carbonization and Liquefaction of Sludge for Harmless and Resource Purposes: A Review, Energy & Fuels 34 (2020) 13268-13290. https://doi.org/10.1021/acs.energyfuels.0c02467

[31] S. Cheng, D. Xing, D.F. Call, B.E. Logan, Direct biological conversion of electrical current into methane by electromethanogenesis, Environ. Sci. Technol. 43 (2009) 3953-3958. https://doi.org/10.1021/es803531g

[32] R. Rodríguez-Alegre, A. Ceballos-Escalera, D. Molognoni , P. Bosch-Jimenez, D. Galí, E. Licon , M.D. Pirriera, J. Garcia-Montaño, E. Borràs, Energies 12 (2019) 361. https://doi.org/10.3390/en12030361

[33] P. Batlle-Vilanova, L. Rovira-Alsina, S. Puig, M. D.Balaguer, P. Icaran, V.M. Monsalvo, F. Rogalla, J. Colprim, Biogas upgrading, CO_2 valorisation and economic revaluation of bioelectrochemical systems through anodic chlorine production in the framework of wastewater treatment plants, Sci. Total Environ. 690 (2019) 352-360. https://doi.org/10.1016/j.scitotenv.2019.06.361.

[34] Y. Wan, Z. Huang, L. Zhou, T. Li, C. Liao, X. Yan, N. Li, X. Wang, Bioelectrochemical Ammoniation Coupled with Microbial Electrolysis for Nitrogen Recovery from Nitrate in Wastewater, Environ Sci Technol. 54 (2020) 3002-3011. https://doi.org/10.1021/acs.est.9b05290

[35] Y.V. Nancharaiah, S. Venkata Mohan, P.N.L. Lens, Recent advances in nutrient removal and recovery in biological and bioelectrochemical systems, Bioresour. Technol. 215 (2016) 173-185. https://doi.org/10.1016/j.biortech.2016.03.129

[36] Y. Ye, H. H. Ngo, W. Guo, Y. Liu, S.W. Chang, D. D. Nguyen, J. Ren, Y. Liu, X. Zhang, Feasibility study on a double chamber microbial fuel cell for nutrient recovery from municipal wastewater, Chem. Eng. J. 358 (2019) 236-242. https://doi.org/10.1016/j.cej.2018.09.215

[37] K. Elmaadawy, B. Liu, J. Hu, H. Hou, J. Yang, Performance evaluation of microbial fuel cell for landfill leachate treatment: Research updates and synergistic effects of hybrid systems. J. Environ. Sci. (China) 96 (2020) 1-20. https://doi.org/10.1016/j.jes.2020.05.005

1131 [38] W. Guo, Y. Ye, H.H. Ngo, Bioelectrochemical System in Wastewater Treatment: Resource
1132 Recovery from Municipal and Industrial Wastewaters, in: W. Guo, H.H. Ngo, R.Y.
1133 Surampalli, T. C. Zhang (Eds.), Sustainable Resource Management, Volume I:
1134 Technologies for Recovery and Reuse of Energy and Waste Materials, I, WILEY-VCH
1135 GmbH. 2021, Weinheim, pp. 489-523.
1136 [39] S. Lu, H. Li, G. Tan, F. Wen, M.T. Flynn, X. Zhu, Resource recovery microbial fuel cells
1137 for urine-containing wastewater treatment without external energy consumption, Chem.
1138 Eng. J. 373 (2019) 1072-1080. https://doi.org/10.1016/j.cej.2019.05.130
1139 [40] A.R. Rahmani, N. Navidjouy, M. Rahimnejad, D. Nematollahi, M. Leili, M. R.
1140 Samarghandi, S. Alizadeh, Application of the eco-friendly bio-anode for ammonium
1141 removal and power generation from wastewater in bio-electrochemical systems, J. Clean.
1142 Prod. 243 (2020) 118589. https://doi.org/10.1016/j.jclepro.2019.118589
1143 [41] M. Qin, Y. Liu, S. Luo, R. Qiao, Z. He, Integrated experimental and modeling evaluation
1144 of energy consumption for ammonia recovery in bioelectrochemical systems, Chem. Eng.
1145 J. 327 (2017) 924-931. https://doi.org/10.1016/j.cej.2017.06.182
1146 [42] A. Almatouq, A.O. Babatunde, Concurrent hydrogen production and phosphorus recovery
1147 in dual chamber microbial electrolysis cell, Bioresour. Technol. 237 (2017) 193-203.
1148 https://doi.org/10.1016/j.biortech.2017.02.043
1149 [43] S. Xu, Y. Zhang, Y. Duan, C. Wang, H. Liu, Simultaneous removal of nitrate/nitrite and
1150 ammonia in a circular microbial electrolysis cell at low C/N ratios, J. Water Process. Eng.
1151 40 (2021) 101938. https://doi.org/10.1016/j.jwpe.2021.101938
1152 [44] M. Zeppilli, M. Simoni, P. Paiano, M. Majone, Two-side cathode microbial electrolysis cell
1153 for nutrients recovery and biogas upgrading, Chem. Eng. J. 370 (2019) 466-476.
1154 https://doi.org/10.1016/j.cej.2019.03.119
1155 [45] C. Santoro, M.J.S. Garcia, X.A. Walter, J. You, P. Theodosiou, I. Gajda, O. Obata, J.
1156 Winfield, J. Greenman, I. Ieropoulos, Urine in Bioelectrochemical Systems: An Overall
1157 Review. ChemElectroChem. 7 (2020)1312-1331. https://doi.org/10.1002/celc.201901995
1158 [46] L. Wang, B. Xie, N. Gao, B. Min, H. Liu, Urea removal coupled with enhanced electricity
1159 generation in single-chambered microbial fuel cells, Environ. Sci. Pollut. Res. 24 (2017)
1160 20401–20408. https://doi.org/10.1007/s11356-017-9689-7
1161 [47] M. Al-Sahari, A. Al-Gheethi, R.M.S.R. Mohamed, E. Noman, M. Naushad, M.B. Rizuan,
1162 D.V. N. Vo, N. Ismail, Green approach and strategies for wastewater treatment using

bioelectrochemical systems: A critical review of fundamental concepts, applications, mechanism, and future trends, Chemosphere 285 (2021) 131373. https://doi.org/10.1016/j.chemosphere.2021.131373

[48] L. Wang, Y. Liu, J. Ma, F. Zhao, Rapid degradation of sulphamethoxazole and the further transformation of 3-amino-5-methylisoxazole in a microbial fuel cell, Water Res. 88 (2016) 322-328. https://doi.org/10.1016/j.watres.2015.10.030

[49] X. Zhang, R. Li, Variation and distribution of antibiotic resistance genes and their potential hosts in microbial electrolysis cells treating sewage sludge. Bioresour. Technol. 315 (2020) 123838. https://doi.org/10.1016/j.biortech.2020.123838

[50] D. Wu, F. Sun, F.J.D. Chua, Y. Zhou, Enhanced power generation in microbial fuel cell by an agonist of electroactive biofilm – Sulfamethoxazole, Chem. Eng. J.384 (2020) 123238. https://doi.org/10.1016/j.cej.2019.123238

[51] B.S. Ondon, S. Li, Q. Zhou, F. Li, Simultaneous removal and high tolerance of norfloxacin with electricity generation in microbial fuel cell and its antibiotic resistance genes quantification, Bioresour. Technol. 304 (2020) 122984. https://doi.org/10.1016/j.biortech.2020.122984

[52] W. Xue, Q. Zhou, F. Li, Bacterial community changes and antibiotic resistance gene quantification in microbial electrolysis cells during long-term sulfamethoxazole treatment, Bioresour. Technol. 294 (2019) 122170. https://doi.org/10.1016/j.biortech.2019.122170

[53] T. Hua, S. Li, F. Li, B.S. Ondon, Y. Liu, H. Wang, Degradation performance and microbial community analysis of microbial electrolysis cells for erythromycin wastewater treatment, Biochem. Eng. J. 146 (2019) 1-9. https://doi.org/10.1016/j.bej.2019.02.008

[54] L. Wang, Y. Liu, C. Wang, X. Zhao, G.D. Mahadeva, Y. Wu, J. Ma, F. Zhao, Anoxic biodegradation of triclosan and the removal of its antimicrobial effect in microbial fuel cells, J. Hazard. Mater. 344 (2018) 669-678. https://doi.org/10.1016/j.jhazmat.2017.10.021

[55] W. Xu, B. Jin, S. Zhou, Y. Su, Y. Zhang, Triclosan Removal in Microbial Fuel Cell: The Contribution of Adsorption and Bioelectricity Generation. Energies. 13 (2020) 761. https://doi.org/10.3390/en13030761

[56] M. Hua, H. He, G. Fu, F. Han, 17b-Estradiol Removal by Electrochemical Technology in the Presence of Electrochemically Active Bacteria in Aerobic Aquatic Environments, Environ. Eng. Sci.36 (2019) 316-325. http://doi.org/10.1089/ees.2018.0331

[57] Q. Zhang, L. Zhang, Z. Li, L. Zhang, D. Li, Enhancement of fipronil degradation with eliminating its toxicity in a microbial fuel cell and the catabolic versatility of anodic biofilm, Bioresour. Technol. 290 (2019) 121723. https://doi.org/10.1016/j.biortech.2019.121723

[58] I. Chakraborty, G.D. Bhowmick, D. Nath, C.N. Khuman, B.K. Dubey, M.M. Ghangrekar, Removal of sodium dodecyl sulphate from wastewater and its effect on anodic biofilm and performance of microbial fuel cell, Int. Biodeter. Biodegradation 156 (2021) 105108. https://doi.org/10.1016/j.ibiod.2020.105108

[59] A.C.J. Tacas, P.-W. Tsai, L. L. Tayo, C.-C. Hsueh, S.-Y. Sun, B.-Y. Chen, Degradation and biotoxicity of azo dyes using indigenous bacteria-acclimated microbial fuel cells (MFCs), Process Biochem. 102 (2021) 59-71. https://doi.org/10.1016/j.procbio.2020.12.003

[60] W. Huang, J. Chen, Y. Hu, L. Zhang, Enhancement of Congo red decolorization by membrane-free structure and bio-cathode in a microbial electrolysis cell, Electrochim. Acta 260 (2018) 196-203. https://doi.org/10.1016/j.electacta.2017.12.055

[61] W. Miran, M. Nawaz, J. Jang, D.S. Lee, Chlorinated phenol treatment and in situ hydrogen peroxide production in a sulfate-reducing bacteria enriched bioelectrochemical system, Water Res. 117 (2017) 198-206. https://doi.org/10.1016/j.watres.2017.04.008

[62] H. Luo, J. Hu, L. Qu, G. Liu, R. Zhang, Y. Lu, J. Qi, J. Hu, C. Zeng, Efficient reduction of nitrobenzene by sulfate-reducer enriched biocathode in microbial electrolysis cell, Sci. Total Environ. 674 (2019) 336-343. https://doi.org/10.1016/j.scitotenv.2019.04.206

[63] Q. Dai, S. Zhang, H. Liu, J. Huang, L. Li, Sulfide-mediated azo dye degradation and microbial community analysis in a single-chamber air cathode microbial fuel cell, Bioelectrochemistry, 131 (2020) 107349. https://doi.org/10.1016/j.bioelechem.2019.107349

[64] D. Cui, M.-H. Cui, B. Liang, W.-Z. Liu, Z.-E. Tang, A.-J. Wang, Mutual effect between electrochemically active bacteria (EAB) and azo dye in bio-electrochemical system (BES), Chemosphere 239 (2020) 124787. https://doi.org/10.1016/j.chemosphere.2019.124787

[65] Y. Hou, L. Tu, S. Qin, Z. Yu, Y. Yan, Y. Xu, H. Song, H. Lin, Y. Chen, S. Wang, Dye wastewater treatment and hydrogen production in microbial electrolysis cells using MoS2-graphene oxide cathode: Effects of dye concentration, co-substrate and buffer solution, Process Biochem. 102 (2021) 51-58. https://doi.org/10.1016/j.procbio.2020.12.008

1226 [66] N. Lu, L. Li, C. Wang, Z. Wang, Y. Wang, Y. Yan, J. Qu, J. Guan, Simultaneous
1227 enhancement of power generation and chlorophenol degradation in nonmodified microbial
1228 fuel cells using an electroactive biofilm carbon felt anode, Sci. Total Environ. 783 (2021)
1229 147045. https://doi.org/10.1016/j.scitotenv.2021.147045
1230 [67] C. Wang, J. Dong, W. Hu, Y. Li, Enhanced simultaneous removal of nitrate and perchlorate
1231 from groundwater by bioelectrochemical systems (BESs) with cathodic potential
1232 regulation, Biochem. Eng. J. 173 (2021) 108068. https://doi.org/10.1016/j.bej.2021.108068
1233 [68] S.R. Kumar, S.A. Patil, Removal of heavy metals using bioelectrochemical systems,
1234 Editor(s): Rouzbeh Abbassi, Asheesh Kumar Yadav, Faisal Khan, Vikram Garaniya,
1235 Integrated Microbial Fuel Cells for Wastewater Treatment, Butterworth-Heinemann, 2020,
1236 Pages 49-71.
1237 [69] Z. Wang, Z. He, Frontier review on metal removal in bioelectrochemical systems:
1238 mechanisms, performance, and perspectives, J. Hazard. Mater. Lett. 1 (2020) 100002.
1239 https://doi.org/10.1016/j.hazl.2020.100002
1240 [70] L. Huang, Z. L., X. Quan, Q. Zhao, W. Yang, B.E. Logan, Efficient in-situ utilization of
1241 caustic for sequential recovery and separation of Sn, Fe, and Cu in microbial fuel cells,
1242 ChemElectroChem 5 (2018) 1658-1669. https://doi.org/10.1002/celc.201800431
1243 [71] G. Pozo, S. Pongy, J. Keller, P. Ledezma, S. Freguia, A novel bioelectrochemical system
1244 for chemical-free permanent treatment of acid mine drainage, Water Res., 126 (2017) 411-
1245 420. https://doi.org/10.1016/j.watres.2017.09.058
1246 [72] S. Gajaraj, X. Sun, C. Zhang, Z. Hu, Improved chromium reduction and removal from
1247 wastewater in continuous flow bioelectrochemical systems. Environ. Sci. Pollut. Res. 26,
1248 31945–31955 (2019). https://doi.org/10.1007/s11356-019-06289-2
1249 [73] M. Li, S. Zhou, Efficacy of Cu(II) as an electron-shuttle mediator for improved
1250 bioelectricity generation and Cr(VI) reduction in microbial fuel cells, Bioresour. Technol.
1251 273 (2019) 122-129. https://doi.org/10.1016/j.biortech.2018.10.074
1252 [74] N. A. D. Ho, S. Babel (2019): Spontaneous reduction of low-potential silver(I)
1253 dithiosulfate complex in bioelectrochemical systems for recovery of silver and
1254 simultaneous electricity production, Environ. Technol. 41 (2020) 3055-3068.
1255 https://doi.org/10.1080/09593330.2019.1597171
1256 [75] X. Song, W. Yang, Z. Lin, L. Huang, X. Quan, A loop of catholyte effluent feeding to
1257 bioanodes for complete recovery of Sn, Fe, and Cu with simultaneous treatment of the co-

present organics in microbial fuel cells, Sci. Total Environ. 651, Part 2 (2019) 1698-1708. https://doi.org/10.1016/j.scitotenv.2018.10.089

[76] S.R.B. Arulmani, J. Dai, H. Li, Z. Chen, H. Zhang, J. Yan, T. Xiao, W. Sun, Efficient reduction of antimony by sulfate-reducer enriched bio-cathode with hydrogen production in a microbial electrolysis cell, Sci. Total Environ. 774 (2021) 145733. https://doi.org/10.1016/j.scitotenv.2021.145733

[77] H. Yu, L. Huang, G. Zhang, P. Zhou, Physiological metabolism of electrochemically active bacteria directed by combined acetate and Cd(II) in single-chamber microbial electrolysis cells, J. Hazard. Mater. 424, Part C (2022) 127538. https://doi.org/10.1016/j.jhazmat.2021.127538

[78] P. Pariyar, K. Kumari, M.K. Jain, P.S. Jadhao, Evaluation of change in biochar properties derived from different feedstock and pyrolysis temperature for environmental and agricultural application, Sci. Total Environ. 713 (2020) 136433. https://doi.org/10.1016/j.scitotenv.2019.136433

[79] M. Alipour, H. Asadi, C. Chen, M.R. Rashti, Bioavailability and eco-toxicity of heavy metals in chars produced from municipal sewage sludge decreased during pyrolysis and hydrothermal carbonization, Ecol. Eng., 162 (2021) 106173. https://doi.org/10.1016/j.ecoleng.2021.106173

[80] C.-S. Liew, W. Kiatkittipong, J.-W. Lim, M.-K. Lam, Y.-C. Ho, C.-D. Ho, S.K.O. Ntwampe, M. Mohamad, A. Usman, Stabilization of heavy metals loaded sewage sludge: Reviewing conventional to state-of-the-art thermal treatments in achieving energy sustainability, Chemosphere, 277 (2021) 130310. https://doi.org/10.1016/j.chemosphere.2021.130310

[81] Y.-C. Chang, X.-F. Xiao, H.-J. Huang, Y.-D. Xiao, H.-S. Fang, J.-B. He, C.-H. Zhou, Transformation characteristics of polycyclic aromatic hydrocarbons during hydrothermal liquefaction of sewage sludge, J. Supercrit. Fluids 170 (2021) 105158. https://doi.org/10.1016/j.supflu.2020.105158

[82] C.A. García, Á. Peña, R. Betancourt, C. A. Cardona, Energetic and environmental assessment of thermochemical and biochemical ways for producing energy from agricultural solid residues: Coffee Cut-Stems case, J. Environ. Manage. 216 (2018) 160-168. https://doi.org/10.1016/j.jenvman.2017.04.029

[83] A.P. Gunasekaran, M.P. Chockalingam, S.R.Padmavathy, J.S. Santhappan, Numerical and experimental investigation on the thermochemical gasification potential of Cocoa pod husk (Theobroma Cacoa) in an open-core gasifier. Clean Technol. Environ. Policy 23 (2021) 1603 - 1615. https://doi.org/10.1007/s10098-021-02051-w

[84] X. Ge, Z. Wu, G. Cravotto, M. Manzoli, P. Cintas, Z. Wu, Cork wastewater purification in a cooperative flocculation/adsorption process with microwave-regenerated activated carbon, J. Hazard. Mater. 360 (2018) 412-419. https://doi.org/10.1016/j.jhazmat.2018.08.022

[85] I. Ibrahim, M.A. Hassan, S. Abd-Aziz, Y. Shirai, Y. Andou, M.R. Othman, A.A. M. Ali, M. R. Zakaria, Reduction of residual pollutants from biologically treated palm oil mill effluent final discharge by steam activated bioadsorbent from oil palm biomass, J. Clean. Prod. 141 (201) 122-127. https://doi.org/10.1016/j.jclepro.2016.09.066

[86] S.S. Lam, M.H. Su, W.L. Nam, D.S. Thoo, C.M. Ng, R.K. Liew, P.N.Y. Yek, N.L. Ma, D.-V.N. Vo, Microwave Pyrolysis with Steam Activation in Producing Activated Carbon for Removal of Herbicides in Agricultural Surface Water, Ind. Eng. Chem. Res. 58 (2018) 695-703. https://doi.org/10.1021/acs.iecr.8b03319

[87] Silvia Escudero-Curiel, Valeria Acevedo-García, Mª Ángeles Sanromán, Marta Pazos, Eco-approach for pharmaceutical removal: Thermochemical waste valorisation, biochar adsorption and electro-assisted regeneration, Electrochim. Acta 389 (2021) 138694. https://doi.org/10.1016/j.electacta.2021.138694

[88] X. Zhou, T.B. Moghaddam, M. Chen, S. Wu, S. Adhikari, Biochar removes volatile organic compounds generated from asphalt, Sci. Total Environ. 745 (2020) 141096. https://doi.org/10.1016/j.scitotenv.2020.141096

[89] K.Vikrant, K.-H. Kim, W. Peng, S. Ge, Y. S. Ok, Adsorption performance of standard biochar materials against volatile organic compounds in air: A case study using benzene and methyl ethyl ketone, Chemical Engineering Journal, 387 (2020) 123943. https://doi.org/10.1016/j.cej.2019.123943

[90] X.J. Lee, L.Y. Lee, S. Gan, S. Thangalazhy-Gopakumar, H. K. Ng, Biochar potential evaluation of palm oil wastes through slow pyrolysis: Thermochemical characterization and pyrolytic kinetic studies, Bioresour. Technol. 236 (2017) 155-163. https://doi.org/10.1016/j.biortech.2017.03.105

[91] K. Xu, F. Lin, X. Dou, M. Zheng, W. Tan, C. Wang, Recovery of ammonium and phosphate from urine as value-added fertilizer using wood waste biochar loaded with magnesium oxides, J. Clean. Prod. 187 (2018) 205-214. https://doi.org/10.1016/j.jclepro.2018.03.206

[92] D.-W. Cho, D.C.W. Tsang, S. Kim, E. E. Kwon, G. Kwon, H. Song, Thermochemical conversion of cobalt-loaded spent coffee grounds for production of energy resource and environmental catalyst, Bioresour. Technol. 270 (2018) 346-351. https://doi.org/10.1016/j.biortech.2018.09.046

[93] B.R. Patra, S. Nanda, A.K. Dalai, V. Meda, Taguchi-based process optimization for activation of agro-food waste biochar and performance test for dye adsorption, Chemosphere 285 (2021) 131531. https://doi.org/10.1016/j.chemosphere.2021.131531

[94] H. Shin, D. Tiwari, D.-J. Kim, Phosphate adsorption/desorption kinetics and P bioavailability of Mg-biochar from ground coffee waste, J. Water Process. Eng. 37 (2020) 101484. https://doi.org/10.1016/j.jwpe.2020.101484

[95] D. Choi, S. Jung, D.-J. Lee, H. Kim, Y. F. Tsang, E. E. Kwon, A new upgrading platform for livestock lignocellulosic waste into syngas using CO2-assisted thermo-chemical process, Energy Convers. Manag.236 (2021) 114084. https://doi.org/10.1016/j.enconman.2021.114084

[96] J.-C. Lin, D. Mariuzza, M. Volpe, L. Fiori, S. Ceylan, J. L. Goldfarb, Integrated thermochemical conversion process for valorizing mixed agricultural and dairy waste to nutrient-enriched biochars and biofuels, Bioresour. Technol. 328 (2021) 124765. https://doi.org/10.1016/j.biortech.2021.124765

[97] J.R. J. Zaeni, J.W. Lim, Z. Wang, D. Ding, Y.S. Chua, S.L. Ng, W.D. Oh, In situ nitrogen functionalization of biochar via one-pot synthesis for catalytic peroxymonosulfate activation: Characteristics and performance studies, Sep. Purif. Technol. 241 (2020) 116702, https://doi.org/10.1016/j.seppur.2020.116702

[98] A.G. Adeniyi, J.O. Ighalo, D.V. Onifade, Biochar from the Thermochemical Conversion of Orange (Citrus sinensis) Peel and Albedo: Product Quality and Potential Applications. Chemistry Africa 3 (2020) 439–448. https://doi.org/10.1007/s42250-020-00119-6

[99] S. Sahota, V.K. Vijay, P.M.V. Subbarao, R. Chandra, P. Ghosh, G. Shah, R. Kapoor, V. Vijay, V. Koutu, I.S. Thakur, Characterization of leaf waste based biochar for cost effective hydrogen sulphide removal from biogas, Bioresour. Technol. 250 (2018) 635-641. https://doi.org/10.1016/j.biortech.2017.11.093

1352 [100] D. Pal, S. K. Maiti, Abatement of cadmium (Cd) contamination in sediment using tea waste
1353 biochar through meso-microcosm study, J. Clean. Prod. 212 (2019) 986-996.
1354 https://doi.org/10.1016/j.jclepro.2018.12.087
1355 [101] S. Keerthanan, A. Bhatnagar, K. Mahatantila, C. Jayasinghe, Y.S. Ok, M. Vithanage,
1356 Engineered tea-waste biochar for the removal of caffeine, a model compound in
1357 pharmaceuticals and personal care products (PPCPs), from aqueous media, Environ.
1358 Technol. Innov. 19 (2020) 100847. https://doi.org/10.1016/j.eti.2020.100847
1359 [102] A. Ashiq, N. M. Adassooriya, B. Sarkar, A.U. Rajapaksha, Y.S. Ok, M. Vithanage,
1360 Municipal solid waste biochar-bentonite composite for the removal of antibiotic
1361 ciprofloxacin from aqueous media, J. Environ. Manage. 236 (2019) 428-435.
1362 https://doi.org/10.1016/j.jenvman.2019.02.006
1363 [103] M. Ayiania, E. Terrell, A. Dunsmoor, F. M. Carbajal-Gamarra, M. Garcia-Perez,
1364 Characterization of solid and vapor products from thermochemical conversion of municipal
1365 solid waste woody fractions, Waste Manage. 84 (2019) 277-285.
1366 https://doi.org/10.1016/j.wasman.2018.11.042
1367 [104] J. Fang, Z. Liu, H. Luan, F. Liu, X. Yuan, S. Long, A. Wang, Y. Ma, Z. Xiao,
1368 Thermochemical liquefaction of cattle manure using ethanol as solvent: Effects of
1369 temperature on bio-oil yields and chemical compositions, Renew. Energy 167 (2021) 32-
1370 41. https://doi.org/10.1016/j.renene.2020.11.033
1371 [105] Q. Wu, H. Wang, X. Zheng, F. Liu, A. Wang, D. Zou, J. Yuan, Z. Xiao, Thermochemical
1372 liquefaction of pig manure: Factors influencing on oil, Fuel 264 (2020) 116884.
1373 https://doi.org/10.1016/j.fuel.2019.116884
1374 [106] S. Zhou, H. Liang, L. Han, G. Huang, Z.Yang, The influence of manure feedstock, slow
1375 pyrolysis, and hydrothermal temperature on manure thermochemical and combustion
1376 properties, Waste Manage. 88 (2019) 85-95. https://doi.org/10.1016/j.wasman.2019.03.025
1377 [107] S. Jung, J.-H. Kim, D.-J. Lee, K.-Y. A. Lin, Y. F. Tsang, M.-H. Yoon, E. E. Kwon, Virtuous
1378 utilization of biochar and carbon dioxide in the thermochemical process of dairy cattle
1379 manure, Chem. Eng. J. 416 (2021) 129110. https://doi.org/10.1016/j.cej.2021.129110
1380 [108] W. Xiang, X. Zhang, K. Chen, J. Fang, F. He, X. Hu, D. C.W. Tsang, Y.S. Ok, B. Gao,
1381 Enhanced adsorption performance and governing mechanisms of ball-milled biochar for
1382 the removal of volatile organic compounds (VOCs), Chem. Eng. J. 385 (2020) 123842.
1383 https://doi.org/10.1016/j.cej.2019.123842

[109] X. Zhang, B. Gao, Y. Zheng, X. Hu, A.E. Creamer, M.D. Annable, Y. Li, Biochar for volatile organic compound (VOC) removal: Sorption performance and governing mechanisms, Bioresour. Technol. 245, Part A (2017) 606-614. https://doi.org/10.1016/j.biortech.2017.09.025

[110] G. Jiang, D. Xu, B. Hao, L. Liu, S. Wang, Z. Wu, Thermochemical methods for the treatment of municipal sludge, J. Clean. Prod. 311 (2021) 127811. https://doi.org/10.1016/j.jclepro.2021.127811

[111] C.I. Aragón-Briceño, A.K. Pozarlik, E.A. Bramer, Lukasz Niedzwiecki, H. Pawlak-Kruczek, G. Brem, Hydrothermal carbonization of wet biomass from nitrogen and phosphorus approach: A review, Renew. Energ. 171 (2021) 401-415. https://doi.org/10.1016/j.renene.2021.02.109

[112] H. Liu, G. Hu, I.A.Basar, J. Li, N. Lyczko, A. Nzihou, C. Eskicioglu, Phosphorus recovery from municipal sludge-derived ash and hydrochar through wet-chemical technology: A review towards sustainable waste management, Chem. Eng. J. 417 (2021) 129300. https://doi.org/10.1016/j.cej.2021.129300

[113] X. Zheng, Y. Ye, Z. Jiang, Z. Ying, S. Ji, W. Chen, B. Wang, B. Dou, Enhanced transformation of phosphorus (P) in sewage sludge to hydroxyapatite via hydrothermal carbonization and calcium-based additive, Sci. Total Environ. 738 (2020) 139786. https://doi.org/10.1016/j.scitotenv.2020.139786

[114] Y. Feng, K. Ma, T. Yu, S. Bai, D. Pei, T. Bai, Q. Zhang, L. Yin, Y. Hu, D. Chen, Phosphorus transformation in hydrothermal pretreatment and steam gasification of sewage sludge, Energy Fuels 32 (2018) 8545-8551. https://doi.org/10.1021/acs.energyfuels.8b01860

[115] G.C. Becker, D. Wüst, H. Köhler, A. Lautenbach, A. Kruse, Novel approach of phosphate-reclamation as struvite from sewage sludge by utilising hydrothermal carbonization, J. Environ. Manage. 238 (2019)119-125. https://doi.org/10.1016/j.jenvman.2019.02.121

[116] Y. Yu, Z. Lei, T. Yuan, Y. Jiang, N. Chen, C. Feng, K. Shimizu, Z. Zhang, Simultaneous phosphorus and nitrogen recovery from anaerobically digested sludge using a hybrid system coupling hydrothermal pretreatment with MAP precipitation, Bioresour. Technol. 243 (2017) 634-640. https://doi.org/10.1016/j.biortech.2017.06.178.

[117] U. Ekpo, A.B. Ross, M.A. Camargo-Valero, L.A. Fletcher, Influence of pH on hydrothermal treatment of swine manure: Impact on extraction of nitrogen and phosphorus

in process water. Bioresour. Technol. 214 (2016) 637-644. https://doi.org/10.1016/j.biortech.2016.05.012

[118] T. Zhang, X. He, Y. Deng, D.C.W. Tsang, H. Yuan, J. Shen, S. Zhang, Swine manure valorization for phosphorus and nitrogen recovery by catalytic–thermal hydrolysis and struvite crystallization, Sci. Total Environ. 729 (2020) 138999. https://doi.org/10.1016/j.scitotenv.2020.138999

[119] L. Dai, B. Yang, H. Li, F. Tan, N. Zhu, Q. Zhu, M. He, Y. Ran, G. Hu, A synergistic combination of nutrient reclamation from manure and resultant hydrochar upgradation by acid-supported hydrothermal carbonization, Bioresour. Technol. 243 (2017) 860-866. https://doi.org/10.1016/j.biortech.2017.07.016

[120] O.P. Crossley, R.B. Thorpe, D. Peus, J. Lee, Phosphorus recovery from process waste water made by the hydrothermal carbonisation of spent coffee grounds, Bioresour. Technol. 301 (2020) 122664. https://doi.org/10.1016/j.biortech.2019.122664